

Fast and Powerful Conditional Randomization Testing via Distillation

Molei Liu^{*1}, Eugene Katsevich², Lucas Janson³, and Aaditya Ramdas⁴

¹Department of Biostatistics, Harvard Chan School of Public Health

²Statistics Department, Wharton School of the University of Pennsylvania

³Department of Statistics, Harvard University

⁴Departments of Statistics & Machine Learning, Carnegie Mellon University

Abstract

We consider the problem of conditional independence testing, where given a response Y and covariates (X, Z) , we test the null hypothesis that $Y \perp\!\!\!\perp X \mid Z$. The conditional randomization test (CRT) was recently proposed as a way to use distributional information about $X \mid Z$ to exactly (non-asymptotically) control Type-I error using *any* test statistic in *any* dimensionality without assuming anything about $Y \mid (X, Z)$. This flexibility in principle allows one to derive powerful test statistics from complex state-of-the-art machine learning algorithms while maintaining statistical validity. Yet the direct use of such advanced test statistics in the CRT is prohibitively computationally expensive, especially with multiple testing, due to the CRT's requirement to recompute the test statistic many times on resampled data. We propose the *distilled CRT*, a novel approach to using state-of-the-art machine learning algorithms in the CRT while drastically reducing the number of times those algorithms need to be run, thereby taking advantage of their power and the CRT's statistical guarantees without suffering the usual computational expense. In addition to distillation, we propose a number of other tricks like screening and recycling computations to further speed up the CRT without sacrificing its high power and exact validity. Indeed, we show in simulations that all our proposals combined lead to a test that has similar power to the CRT but requires orders of magnitude less computation, making it a practical tool even for large data sets. We demonstrate these benefits on a breast cancer dataset by identifying biomarkers related to cancer stage.

Keywords: Conditional Randomization Test (CRT), model-X, conditional independence testing, high-dimensional inference, machine learning.

1 Introduction

In our increasingly data-driven world, it has become the norm in applications from genetics and health care to policy evaluation and e-commerce to seek to understand the relationship between a response variable of interest and a high-dimensional set of potential explanatory variables or covariates. While accurately estimating this entire relationship generally would require a nearly-infinite sample size, a less-intractable but still extremely useful question is to ask, for any given covariate, whether it actually contributes to the response variable's high-dimensional conditional

^{*}This paper is a post-hoc merge of two parallel works by Liu & Janson (2020) and Katsevich & Ramdas (2020).

distribution. We address this problem by encoding a covariate’s relevance in *conditional independence testing*, which requires no modeling assumptions to define. Denoting the response random variable by Y , a given covariate of interest by X , and a multidimensional set of further covariates by $Z = (Z_1, \dots, Z_p)$, the null hypothesis we seek to test is

$$H_0 : Y \perp\!\!\!\perp X \mid Z$$

against the alternative $H_1 : Y \not\perp\!\!\!\perp X \mid Z$. Testing this hypothesis for just a single covariate is sometimes all that is needed, such as in an observational study investigating whether a particular treatment (X) causes a change in a response (Y) after controlling for a set of measured confounding variables (Z). But in other applications no one covariate holds *a priori* precedence over another, and a researcher seeks any and all covariates that contribute to Y ’s conditional distribution. This variable selection objective can also be achieved by testing H_0 for each covariate in turn and plugging the resulting p -values into one of the many procedures from the extensive literature on multiple testing. In addition to the considerable statistical challenge of providing a valid and powerful test of H_0 , it is of paramount importance to also ensure that test is computationally efficient, especially, as is often the case in modern applications, when either or both the sample size and dimension are large, and even more so when a variable selection objective requires the test to be run many times. Thus the goal of this paper is to present a test for conditional independence that is provably valid, empirically powerful, and computationally efficient.

1.1 Background

Our work builds on the *conditional randomization test* (CRT) introduced in Candès et al. (2018). The CRT is a very general framework for conditional independence testing that can leverage any test statistic one chooses and exactly (non-asymptotically) controls the Type-I error regardless of the data dimensionality. The CRT’s guarantees assume nothing whatsoever about $Y \mid (X, Z)$, but instead assume $X \mid Z$ is known. This so-called “model- X ” framework (in contrast to the canonical approach of assuming a strong model for $Y \mid (X, Z)$) is perhaps easiest to justify when a wealth of *unlabeled data* (pairs (X_i, Z_i) without corresponding Y_i) is available, but has also been found to be quite robust even when $X \mid Z$ is estimated by only the labeled data.

In order to define the CRT, we first need notation for our data. For $i \in \{1, \dots, n\}$, let $(Y_i, X_i, Z_i) \in \mathbb{R}^{p+2}$ be i.i.d. copies of (Y, X, Z) , and denote the column vector of Y_i ’s by $\mathbf{y} \in \mathbb{R}^n$, the column vector of X_i ’s by $\mathbf{x} \in \mathbb{R}^n$, and the matrix whose rows are the Z_i ’s by $\mathbf{Z} \in \mathbb{R}^{n \times p}$. The CRT is given by Algorithm 1, and its Type-I error guarantee follows below.

Algorithm 1 The conditional randomization test (CRT).

Input: Data $(\mathbf{y}, \mathbf{x}, \mathbf{Z})$, test statistic function T , and number of randomizations M .

for $m = 1, 2, \dots, M$ **do**

Sample $\mathbf{x}^{(m)}$ from the distribution of $\mathbf{x} \mid \mathbf{Z}$, conditionally independently of \mathbf{x} and \mathbf{y} .

end for

Output: CRT p -value $p(\mathbf{X}, \mathbf{y}) = \frac{1}{M+1} \left(1 + \sum_{m=1}^M \mathbb{1}_{\{T(\mathbf{y}, \mathbf{x}^{(m)}, \mathbf{Z}) \geq T(\mathbf{y}, \mathbf{x}, \mathbf{Z})\}} \right)$.

Theorem 1 (Candès et al. (2018)). *The CRT p -value $p(\mathbf{X}, \mathbf{y})$ satisfies $\mathbb{P}_{H_0}(p(\mathbf{X}, \mathbf{y}) \leq \alpha) \leq \alpha$ for all $\alpha \in [0, 1]$.*

For many common models of $X \mid Z$, the conditionally-independent sampling of $\mathbf{x}^{(m)}$ is straightforward. And even in more complex models it is still often easy to sample $\mathbf{x}^{(m)}$ conditionally-exchangeably with \mathbf{x} and conditionally-independently of \mathbf{y} (for instance by conditioning on an

inferred latent variable), which is sufficient for Theorem 1 to hold. Because Theorem 1 only relies on the exchangeability of the vectors $\mathbf{x}, \mathbf{x}^{(1)}, \dots, \mathbf{x}^{(M)}$ under H_0 , it is entirely agnostic to the choice of test statistic T . This enables some very powerful choices, such as T 's derived from modern machine learning algorithms, from Bayesian inference (though neither the prior nor model for $Y \mid (X, Z)$ need be well-specified), or from highly domain-specific knowledge or intuition. Unfortunately the most powerful statistics are often particularly expensive to compute, and as can be seen from Algorithm 1, T must be applied $M + 1$ times in order to compute a single p -value. When testing all the covariates at once, this computational problem is compounded as not only does *each* test require $M + 1$ applications of T , but M must be roughly of order p to ensure the p -values are sufficiently high-resolution to make any discoveries with standard multiple testing procedures such as Benjamini–Hochberg (Benjamini and Hochberg, 1995).

1.2 Our contribution

We resolve this computational challenge in Section 2 by introducing a technique we call *distillation* to the CRT that can still leverage *any* high-dimensional modeling or supervised learning algorithm, but presents dramatic computational savings by only requiring the expensive high-dimensional computation to be performed once, instead of $M + 1$ times. We call our proposed method the distilled CRT, or dCRT, and show how to further improve its computation in multiple testing settings in Section 3.

We demonstrate in simulations in Section 4 that there is generally little or no power loss when comparing the dCRT to its more expensive CRT counterpart, while our proposals save orders of magnitude in computation even for medium-scale problems (the savings only increase for larger data). We also show in simulations that the dCRT is comparably powerful to other state-of-the-art conditional independence tests, and is also robust to misspecification in the distribution of X .

In Section 5, we apply the dCRT to a breast cancer dataset and discover more clinically-informative somatic mutations than competing methods, and we cite independent scientific work corroborating each of the discoveries we make. Finally, we close with a discussion in Section 6.

The dCRT inherits several attractive properties of the CRT: it is an essentially non-randomized procedure that yields finite-sample valid p -values for all variables that can be used for downstream multiple testing analyses with a variety of target error rates, including not only the false discovery rate (FDR) but also the family-wise error rate (FWER) and others. This makes the dCRT an appealing alternative to model-X knockoffs (Candès et al., 2018).

1.3 Related work

Our work builds upon the CRT of Candès et al. (2018), with the goal of making it computationally tractable without sacrificing power. Our work is perhaps most similar in its goal to the HRT of Tansey et al. (2018), which uses data splitting to enable the use of complex modeling in the CRT with far less computation by doing all the complex modeling on the first part of the data and testing on the second part. A similar approach is adopted in Bates et al. (2020), who apply the CRT to genetic trio studies, and another sample-splitting extension of the HRT is introduced in Katsevich and Ramdas (2020b) to enable power analysis. We show in Section 4 that data splitting comes with a substantial power loss compared to the dCRT and the original (slower) CRT. Tansey et al. (2018) addresses this with cross-fitting, but in doing so loses the guarantee on Type-I error control of the CRT (and dCRT). Other works have extended the CRT (Berrett et al., 2019; Bellot and van der Schaar, 2019) in ways that do not address its computational intractability. For the variable selection problem, model-X knockoffs (Candès et al., 2018) can simultaneously test conditional

independence for each covariate, yielding an FDR-controlling rejection set. Model-X knockoffs is focused on a narrower problem (e.g., unlike CRT, it is not designed to test the significance of a single variable), but it is a powerful solution to this problem. We revisit this comparison in the discussion.

We note a pair of methods, double machine learning (DML) (Chernozhukov et al., 2016) and the generalized covariance measure (GCM) (Shah and Peters, 2018), that both test conditional independence under assumptions that nearly (but not quite, due to moment conditions on Y) subsume ours, and whose test statistic resembles and can even be identical to certain special cases of the dCRT. However, their statistics only resemble a special case of the dCRT—the dCRT framework includes many other statistics which deviate substantially from DML/GCM and can be more powerful in certain settings. Furthermore, the cutoffs for their test statistics are both based on asymptotic normality, while the dCRT is non-asymptotically exact regardless of the distribution of its test statistic (see Appendix D.4).

1.4 Notation

Let $I = (i_1, i_2, \dots, i_k) \subseteq \{1, \dots, n\}$ and $J = (j_1, j_2, \dots, j_\ell) \subseteq \{1, 2, \dots, p\}$ be subsets of samples and variables, respectively, and consider a matrix $\mathbf{A} = (\mathbf{a}_1, \mathbf{a}_2, \dots, \mathbf{a}_p) \in \mathbb{R}^{n \times p}$ with $\mathbf{a}_j = (A_{1j}, A_{2j}, \dots, A_{nj})^\top$. We denote by $A_{I,J}$ the sub-matrix of A with rows in I and columns in J . We use the subscripts j , $-J'$, and \bullet as shorthand for $J = \{j\}$, $\{1, \dots, p\} \setminus J'$, and $\{1, \dots, p\}$, respectively, and the same for the first index. For example, $A_{\bullet,-j}$ represents the matrix A with the j th column removed. For any two vectors \mathbf{a}_j and \mathbf{a}_ℓ , let $\mathbf{a}_j \odot \mathbf{a}_\ell = (A_{1j}A_{1\ell}, A_{2j}A_{2\ell}, \dots, A_{nj}A_{n\ell})^\top$ denote their elementwise product, and for $L = \{\ell_1, \ell_2, \dots, \ell_k\}$ let $\mathbf{a}_j \odot \mathbf{A}_L = (\mathbf{a}_j \odot \mathbf{a}_{\ell_1}, \dots, \mathbf{a}_j \odot \mathbf{a}_{\ell_k})$; these will be used when fitting first-order interaction effects.

2 The distilled conditional randomization test

2.1 Main idea

It is natural to derive CRT test statistics from machine learning methods with high predictive and estimation accuracy. Indeed the original paper proposing the CRT (Candès et al., 2018) used the lasso (Tibshirani, 1996) to derive a test statistic and found it to be quite powerful. Specifically, the test statistic was chosen to be $T_{\text{CRT}}(\mathbf{y}, \mathbf{x}, \mathbf{Z}) := |\hat{\beta}_x|$, the absolute value of the fitted coefficient on \mathbf{x} from the lasso of \mathbf{y} on (\mathbf{x}, \mathbf{Z}) with penalty parameter chosen by cross-validation. Although powerful and computationally much faster than many other machine learning algorithms, it is still expensive to repeatedly run the lasso on large data sets hundreds or more times just to compute a single p -value, and many times more than that in multiple-testing scenarios when a p -value for each covariate is needed.

Consider now the following alternative test statistic which captures the essence of our proposal. First fit a cross-validated lasso of \mathbf{y} on \mathbf{Z} to obtain the p -dimensional coefficient vector $\hat{\beta}_{\mathbf{Z}}$. Then fit a least-squares regression of the residual $(\mathbf{y} - \mathbf{Z}\hat{\beta}_{\mathbf{Z}})$ on \mathbf{x} to obtain the scalar coefficient $\hat{\beta}'_x$ and take its absolute value $T_{\text{dCRT}}(\mathbf{y}, \mathbf{x}, \mathbf{Z}) := |\hat{\beta}'_x|$ as the test statistic. It may seem as though little has changed from the preceding paragraph—we would expect T_{CRT} and T_{dCRT} to have similar statistical properties and require nearly the same computation. Although the statistical properties of T_{CRT} and T_{dCRT} are indeed very similar and they do require nearly the same time to compute *once*, they require dramatically different computation within the CRT. The key difference is that the expensive $(p+1)$ -dimensional lasso fit in T_{CRT} must be recomputed for *each* resample of \mathbf{x} , while the expensive p -dimensional lasso fit in T_{dCRT} must only be computed once, since that lasso

does not depend on \mathbf{x} and hence is identical for all its resamples. In the CRT, neither \mathbf{y} nor \mathbf{Z} change during the resampling procedure, and we take advantage of this by applying our expensive computation to only \mathbf{y} and \mathbf{Z} so it only has to be done once. All that is required for each resample’s computation of T_{dCRT} is a *univariate* regression, whose computational expense is much lower than a p -dimensional lasso.

We can generalize this idea far beyond the lasso or linear regressions. The core proposal is to *distill* all the high-dimensional information in \mathbf{Z} about \mathbf{y} into a low-dimensional representation, without looking at \mathbf{x} . Then the test statistic estimates a relationship between \mathbf{x} and the *leftover* information in \mathbf{y} by only looking at \mathbf{x} , \mathbf{y} , and the distilled (low-dimensional) function of \mathbf{Z} . Thus all the computation on high-dimensional data, namely the distillation, only needs to be performed once, while the computation that is repeatedly applied to the resampled data is low-dimensional and hence relatively fast. It will often be advantageous to also distill the high-dimensional information in \mathbf{Z} about \mathbf{x} and include this in the test statistic as well, but we will see this can be done without looking at \mathbf{x} and hence does not require any repeated computation on the resampled $\mathbf{x}^{(m)}$.

2.2 Formal presentation of dCRT

We now formalize the idea from the previous subsection in Algorithm 2, the distilled conditional randomization test (dCRT).

Algorithm 2 The distilled conditional randomization test (dCRT).

Input: Data $(\mathbf{y}, \mathbf{x}, \mathbf{Z})$, \mathbf{y} -distillation-fitting function \mathcal{D}_y , \mathbf{x} -distillation function d_x , test statistic function T , and number of randomizations M .

Distill \mathbf{Z} ’s information about \mathbf{y} into $\mathbf{d}_y = \mathcal{D}_y(\mathbf{y}, \mathbf{Z})$ and about \mathbf{x} into $\mathbf{d}_x = d_x(\mathbf{Z})$.

for $m = 1, 2, \dots, M$ **do**

 Sample $\mathbf{x}^{(m)}$ from the distribution of $\mathbf{x} \mid \mathbf{Z}$, conditionally independently of \mathbf{x} and \mathbf{y} .

end for

Output: dCRT p -value $\frac{1}{M+1} \left(1 + \sum_{m=1}^M \mathbb{1}_{\{T(\mathbf{y}, \mathbf{x}^{(m)}, \mathbf{d}_y, \mathbf{d}_x) \geq T(\mathbf{y}, \mathbf{x}, \mathbf{d}_y, \mathbf{d}_x)\}} \right)$.

The key difference from the more general CRT in Algorithm 1 is that the test statistic function T in Algorithm 2 only sees information about the high-dimensional \mathbf{Z} through its \mathbf{y} - and \mathbf{x} -distillations \mathbf{d}_y and \mathbf{d}_x , which are both computed just once in the first line of the algorithm. \mathcal{D}_y and d_x should be chosen such that the distillation step produces \mathbf{d}_y and \mathbf{d}_x with dimension much less than p , so that T ’s inputs are low-dimensional. Then since T is the only repeatedly-applied function and its computation does not suffer from the high-dimensionality of the original data, the dCRT’s computation will be dominated by the single application of \mathcal{D}_y . For instance, in the dCRT example in Section 2.1, \mathbf{d}_x is not used and \mathcal{D}_y fits a cross-validated lasso of \mathbf{y} on \mathbf{Z} and returns $\mathbf{d}_y = \mathbf{Z}\hat{\beta}_z$, while $T(\mathbf{y}, \mathbf{x}, \mathbf{d}_y) = (\mathbf{y} - \mathbf{d}_y)^\top \mathbf{x} / \|\mathbf{x}\|^2$ requires negligible computation by comparison.

Note that \mathcal{D}_y and d_x , despite both producing distillations, operate quite differently. In particular, although d_x distills \mathbf{Z} ’s information about \mathbf{x} , it does not take \mathbf{x} as an argument. This is because the distillation function d_x can be chosen purely based on $X \mid Z$ which is assumed known, and thus can bypass looking at \mathbf{x} and distill \mathbf{Z} directly; for example, we will soon discuss dCRTs with $d_x(z) = \mathbb{E}[\mathbf{x} \mid \mathbf{Z} = z]$. In contrast, \mathcal{D}_y needs to internally *fit* a distillation function which we could think of as “ d_y ” (this is the expensive step) and then apply it to \mathbf{Z} to compute \mathbf{d}_y . This distinction between \mathcal{D}_y and d_x is important since if d_x performed a complicated fitting step that depended on \mathbf{x} , then that complicated computation would have to be repeated for each $\mathbf{x}^{(m)}$ in order to maintain

the exchangeability of $\mathbf{x}, \mathbf{x}^{(1)}, \dots, \mathbf{x}^{(M)}$ under H_0 used in the proof of Theorem 1. Importantly, Theorem 1’s validity guarantee indeed applies to the dCRT because it is a computationally efficient instantiation of (and thus a special case of) the CRT.

We emphasize that \mathcal{D}_y can really be *any* regression algorithm and Theorem 1 still holds. Thus it can take advantage of the predictive power of state-of-the-art machine learning algorithms, precise knowledge in the form of a Bayesian prior, or even imprecise domain expertise or intuition applied by trying many different regressions of \mathbf{y} on \mathbf{Z} and choosing whichever “feels” best (as long as \mathbf{x} is not factored into that decision). In the sequel we provide some suggestions and default choices.

2.3 Specific constructions of the dCRT

Algorithm 2 provides a framework for fast and powerful CRTs, but leaves much unspecified. In this section, we provide more detail on some ways that the dCRT can be implemented in different scenarios, and discuss their associated advantages and disadvantages.

2.3.1 The d₀CRT: fast, powerful, and intuitive

The most computationally-efficient and intuitive class of dCRT procedures has both \mathbf{y} - and \mathbf{x} -distillations reduce \mathbf{Z} to an output with a single column. We label this subclass of dCRT procedures as d₀CRT because it represents the choice to maximally-distill each row of \mathbf{Z} down to a single scalar. Assuming T ’s computation generally increases with the dimension of its inputs, the d₀CRT also represents a particularly computationally-efficient class of dCRTs.

A natural approach to constructing a d₀CRT, especially when Y is continuous, is to have distillation take the form of conditional mean functions. That is, let $d_x(\mathbf{Z}) = \mathbb{E}[\mathbf{x} | \mathbf{Z}]$ and have \mathcal{D}_y fit an estimate of the analogous regression function for \mathbf{y} , i.e., $\mathcal{D}_y(\mathbf{y}, \mathbf{Z}) \approx \mathbb{E}[\mathbf{y} | \mathbf{Z}]$. Then T can be chosen as an empirical measure of dependence between the residuals $\mathbf{y} - \mathbf{d}_y$ and $\mathbf{x} - \mathbf{d}_x$, such as the square of the fitted coefficient when regressing the former on the latter. This approach is also easy to understand and implement since it just requires choosing \mathcal{D}_y and T , with \mathcal{D}_y just performing a (possibly nonparametric) regression while T can be thought of as computing a test statistic for testing the independence between two scalar random variables from a paired sample of size n : $(\mathbf{y} - \mathbf{d}_y, \mathbf{x} - \mathbf{d}_x)$. As both regression and bivariate independence testing are highly-studied topics, users can easily draw from their statistical training, domain expertise, and a rich literature in order to design an appropriate d₀CRT for their particular problem. As a generic example we found to be computationally efficient and powerful in our simulations, consider the following.

Example 1 (lasso-based d₀CRT). Let $\mathbf{d}_y = \mathbf{Z}\hat{\beta}_z$ be the fitted predictions from a cross-validated lasso of \mathbf{y} on \mathbf{Z} , let $\mathbf{d}_x = \mathbb{E}[\mathbf{x} | \mathbf{Z}]$, and let $T(\mathbf{y}, \mathbf{x}, \mathbf{d}_y, \mathbf{d}_x) = \hat{\beta}_x^2 := \left(\frac{(\mathbf{y} - \mathbf{d}_y)^\top (\mathbf{x} - \mathbf{d}_x)}{\|\mathbf{x} - \mathbf{d}_x\|^2} \right)^2$.

In spite of the intuitive appeal of couching distillation in terms of finding conditional means, in some problem instances an alternative d₀CRT may be more appropriate. For instance, an appealing analogue of Example 1 for binary Y might fit $\hat{\beta}_z$ by a cross-validated L_1 -penalized logistic regression of \mathbf{y} on \mathbf{Z} and otherwise leave \mathcal{D}_y and \mathbf{d}_x unchanged (note $\mathbf{Z}\hat{\beta}_z$ no longer approximates $\mathbb{E}[\mathbf{y} | \mathbf{Z}]$), and take $T(\mathbf{y}, \mathbf{x}, \mathbf{d}_y, \mathbf{d}_x)$ to be the squared fitted coefficient from a logistic regression of \mathbf{y} on $\mathbf{x} - \mathbf{d}_x$ with offset \mathbf{d}_y . The substantial flexibility of the d₀CRT allows it to detect many kinds of nonlinear relationships between Y and X , but the stringent distillation inherently limits its ability to detect most types of *interactions* between X and Z . This shortcoming can be important and in the next subsection we discuss how interactions can be incorporated by moving beyond the d₀CRT.

2.3.2 The d₁CRT: accounting for interactions

Of the three functions applied in Algorithm 2, only T takes both \mathbf{y} and \mathbf{x} as arguments and hence the choice of T is how a user can encode the kinds of non-null relationships between Y and X that are deemed plausible. But because T only sees \mathbf{Z} through \mathbf{d}_y and \mathbf{d}_x , any plausible models for Y must be expressed using only \mathbf{x} , \mathbf{d}_y , and \mathbf{d}_x . This means in particular that the d₀CRT has almost no capacity to model even first-order interactions between X and Z . For instance, suppose $p = 3$ and $Z_j \stackrel{i.i.d.}{\sim} \mathcal{N}(0, 1)$, $X \sim Z_1 + \mathcal{N}(0, 1)$, and $Y \sim Z_2 + XZ_3 + \mathcal{N}(0, 1)$. Then the best possible distillations of \mathbf{x} and \mathbf{y} are $\mathbf{d}_x = \mathbf{Z}_1$ and $\mathbf{d}_y = \mathbf{Z}_2 + \mathbf{Z}_1 \odot \mathbf{Z}_3$, respectively, making it impossible for T to encode the true conditional mean of \mathbf{y} , namely, $\mathbf{Z}_2 + \mathbf{x} \odot \mathbf{Z}_3$, from just \mathbf{x} , \mathbf{d}_x , and \mathbf{d}_y .

To address this limitation of the d₀CRT, one can simply increase the dimension of \mathbf{d}_y and \mathbf{d}_x to explicitly include possible columns of \mathbf{Z} with which \mathbf{x} might be expected to interact. But of course increasing the dimension of \mathbf{d}_y and \mathbf{d}_x tends to come at a computational cost, since their low-dimensionality is exactly what makes the dCRT fast in the first place. Thus one needs some sort of prior, domain knowledge, or heuristic for choosing based on either the pair (\mathbf{y}, \mathbf{Z}) or (\mathbf{x}, \mathbf{Z}) (but not based on $(\mathbf{y}, \mathbf{x}, \mathbf{Z})$ together) a small subset of columns of \mathbf{Z} that \mathbf{x} might plausibly interact with. One option is to split the data into two independent parts and use one part in an unconstrained way to select columns of \mathbf{Z} that are likely to interact with \mathbf{x} , and then to leverage these selections in a dCRT run only on the other part. We propose here an alternative that avoids sample splitting, based on the common statistical practice of only allowing for interactions between variables with strong main effects. This practice of enforcing hierarchy in interactions has a long history in applied and theoretical statistics under many different names (Nelder, 1977; Cox, 1984; Peixoto, 1987; Hamada and Wu, 1992; Chipman, 1996; Bien et al., 2013).

Our proposed method for incorporating interactions, which we call the d₁CRT, is to have \mathcal{D}_y still distill \mathbf{Z} into one column to best-capture the relationship between \mathbf{y} and \mathbf{Z} , but then to additionally return (as further columns of \mathbf{d}_y) a limited subset of columns of \mathbf{Z} whose contributions to that fitted relationship are strongest. Then T can be chosen as a test statistic that allows \mathbf{x} to interact with those columns of \mathbf{Z} contained in \mathbf{d}_y , while still prioritizing the main effect of \mathbf{x} . As a generic example we found to be powerful to detect hierarchical interactions without losing much power in the absence of interactions, consider the following.

Example 2 (lasso-based d₁CRT). Let $\mathbf{d}_y = (\mathbf{Z}\hat{\beta}_z, \mathbf{Z}_{\bullet, \text{top}(k)}) := (\mathbf{d}_{y,1}, \mathbf{d}_{y,-1})$ be the fitted predictions from a cross-validated lasso of \mathbf{y} on \mathbf{Z} concatenated with the columns of \mathbf{Z} corresponding to the k largest entries of $|\hat{\beta}_z|$, let $\mathbf{d}_x = \mathbb{E}[\mathbf{x} | \mathbf{Z}]$, and let $T(\mathbf{y}, \mathbf{x}, \mathbf{d}_y, \mathbf{d}_x) = \hat{\beta}_{x,1}^2 + \frac{1}{k} \sum_{j=2}^{k+1} \hat{\beta}_{x,j}^2$, where $\hat{\beta}_x \in \mathbb{R}^{k+1}$ are the fitted coefficients from a least-squares fit of $(\mathbf{y} - \mathbf{d}_{y,1})$ on $(\mathbf{x} - \mathbf{d}_x)$ and $(\mathbf{x} - \mathbf{d}_x) \odot \mathbf{d}_{y,-1}$.

The normalization by $1/k$ of $\sum_{j=2}^{k+1} \hat{\beta}_{x,j}^2$ encodes our hierarchical prioritization of the main effect $\hat{\beta}_{x,1}$ over the interaction effects. For small k we still expect the computation to be dominated by \mathcal{D}_y , but it also represents a statistical trade-off in how widely to search for interactions; we found the performance to be quite stable to k in our simulations, but set as a default $k = 2 \log(p)$. Note that k could also be chosen after looking at (\mathbf{y}, \mathbf{Z}) , and more generally, one can construct many different types of d₁CRT. For instance, one can adapt Example 2 to binary Y in an analogous way as was done for Example 1 by replacing linear regressions with logistic regressions and using $\mathbf{d}_{y,1}$ as an offset in T . Or one could have \mathcal{D}_y and/or T use the predictions and default variable importance measures from a random forest. We explore some of these options in simulations in Section 4.

2.4 Running the dCRT without resampling

Distillation massively reduces the computation time of the CRT by only requiring a single evaluation of the by-far-most-expensive function \mathcal{D}_y . But it still requires $M + 1$ evaluations of T , which can sometimes still contribute nontrivially to the computation time, and requires the user to choose the tuning parameter M which trades off computation and statistical power. It turns out that in certain cases the simplicity of T in the dCRT can be leveraged to remove the resampling of $\mathbf{x}^{(m)}$ entirely and compute an exact p -value directly from the single function evaluation $T(\mathbf{y}, \mathbf{x}, \mathbf{d}_y, \mathbf{d}_x)$.

For intuition, suppose $X | Z \sim \mathcal{N}(Z^\top \beta, \sigma^2)$, and consider the d_0 CRT with T as in Example 1,

$$T(\mathbf{y}, \mathbf{x}, \mathbf{d}_y, \mathbf{d}_x) = \left(\frac{(\mathbf{y} - \mathbf{d}_y)^\top (\mathbf{x} - \mathbf{d}_x)}{\|\mathbf{x} - \mathbf{d}_x\|^2} \right)^2.$$

Then since the (d)CRT conditions on \mathbf{y} and \mathbf{Z} (and hence also \mathbf{d}_y and $\mathbf{d}_x = \mathbf{Z}\beta$),

$$(\mathbf{y} - \mathbf{d}_y)^\top (\mathbf{x} - \mathbf{d}_x) \sim \mathcal{N}\left(0, \sigma^2 \|\mathbf{y} - \mathbf{d}_y\|^2\right).$$

The denominator of T makes things a bit more complicated, but the nature of the statistic does not change much if we replace the denominator by its expectation or, equivalently (since multiplying T by a fixed constant has no effect on its resulting p -value), simply replace it by 1: $T'(\mathbf{y}, \mathbf{x}, \mathbf{d}_y, \mathbf{d}_x) = \left((\mathbf{y} - \mathbf{d}_y)^\top (\mathbf{x} - \mathbf{d}_x) \right)^2$. We then get immediately that the *exact* p -value (i.e., the p -value that would result from taking the limit as $M \rightarrow \infty$) can be computed as $2 \left(1 - \Phi \left(\frac{\sqrt{T'(\mathbf{y}, \mathbf{x}, \mathbf{d}_y, \mathbf{d}_x)}}{\sigma \|\mathbf{y} - \mathbf{d}_y\|} \right) \right)$ without ever resampling $\mathbf{x}^{(m)}$ or recomputing T' , where Φ is the standard normal CDF.

The same principle can be applied to non-Gaussian X : since the distribution of $(\mathbf{x} - \mathbf{d}_x) | \mathbf{Z}$ is known and the rows are independent, $(\mathbf{x} - \mathbf{d}_x)$ can be element-wise transformed via scalar monotone functions to be i.i.d. $\mathcal{N}(0, 1)$ given \mathbf{Z} . For conditionally-continuously-distributed $(\mathbf{x} - \mathbf{d}_x)$, this can be done via the probability inverse transform, while for distributions with atoms the atoms need to be carefully randomized (though just once); see Appendix A for details.

As long as $(\mathbf{x} - \mathbf{d}_x)$ is independent Gaussian or transformed to be, the same principle can also be applied to some more complex T functions. For instance, in Example 2, we can again replace the random “denominator” (in this case the matrix inverse in the least-squares formula for $\hat{\beta}_x$) with its conditional expectation given \mathbf{Z} , and end up with a quadratic form in Gaussian random variables. Efficient algorithms for computing the quantiles of a quadratic form in Gaussian random variables exist (Duchesne and De Micheaux, 2010) and can be applied to again compute the exact dCRT p -value without any resampling; see Appendix A for details.

3 Variable selection and multiple testing via the dCRT

Conditional independence testing is often done in the context of a variable selection problem. Given p covariates X_1, \dots, X_p and a response Y , the goal is to discover the covariates X_j that are conditionally associated with the response, i.e., $Y \not\perp X_j | X_{-j}$. For a given j , we arrive at the problem formulation from the previous two sections by setting $X = X_j$ and $Z = X_{-j}$. This change of notation highlights the fact that the effects of all variables are of interest, rather than that of one special variable. Given a design matrix $\mathbf{X} \in \mathbb{R}^{n \times p}$ and a response vector \mathbf{y} , we propose to approach the variable selection problem by applying the dCRT to $(\mathbf{y}, \mathbf{x}, \mathbf{Z}) = (\mathbf{y}, \mathbf{X}_{\bullet, j}, \mathbf{X}_{\bullet, -j})$ for each covariate j , followed by a multiple testing procedure on the resulting p -values. Two common

error rates to control are the family-wise error rate (FWER) and the false discovery rate (FDR). The former can be easily achieved based on the Bonferroni correction, which works under arbitrary p -value dependence. The latter is usually done via the Benjamini–Hochberg procedure. Even though the p -values are technically not positively dependent in the sense required for mathematical FDR control (Benjamini and Yekutieli, 2001), the Benjamini–Hochberg procedure is known to be very robust to dependent p -values in all but adversarially-constructed settings, as confirmed in our simulations.

Regardless of error rate, the straightforward application of the dCRT to the variable selection problem requires computing \mathcal{D}_y a total of p times, once for each variable. Note that these are entirely parallel computations, so for certain problem dimensionalities and parallel computing resources, this is entirely feasible. However, in large-scale variable selection applications such as genome-wide association studies, there may be too many covariates for the direct application of dCRT to each. In the following subsections we present two computational shortcuts that make variable selection via the dCRT feasible for large-scale applications.

3.1 Data-dependent screening of variables

A natural acceleration of the dCRT for variable selection is to first use the data to identify a preliminary subset $\mathcal{S} \subseteq \{1, \dots, p\}$ of promising covariates via a screening function $S : (\mathbf{X}, \mathbf{y}) \mapsto \mathcal{S}$. We can then compute (d)CRT p -values $p_j(\mathbf{X}, \mathbf{y})$ for only $j \in \mathcal{S}$ while setting the p -values for all the other covariates to 1, yielding the screened p -values

$$p'_j(\mathbf{X}, \mathbf{y}) = \begin{cases} p_j(\mathbf{X}, \mathbf{y}) & \text{if } j \in S(\mathbf{X}, \mathbf{y}); \\ 1 & \text{if } j \notin S(\mathbf{X}, \mathbf{y}). \end{cases} \quad (1)$$

For instance, \mathcal{S} could be the active set of a cross-validated lasso fit of \mathbf{y} on all the covariates.

Unfortunately, in general, a screening step like this applied before the (d)CRT breaks the exchangeability between the original and resampled test statistics which Theorem 1 relies on to guarantee p -value validity. The intuitive reason for the failure of exchangeability is that the screening, when it discards covariates, takes a (data-dependent, and thus random) subset of covariates and implicitly changes their (d)CRT test statistics to ensure a p -value of 1 is returned. Hence, the screening implies an \mathbf{x} -dependent choice of T , whose distribution under the null will then be different when its argument is \mathbf{x} versus $\mathbf{x}^{(m)}$. Despite this failure of exchangeability, the screening can only inflate a p -value and thus does not affect its validity. Indeed, since $p_j(\mathbf{X}, \mathbf{y}) \leq p'_j(\mathbf{X}, \mathbf{y})$, the validity of the CRT p -value $p_j(\mathbf{X}, \mathbf{y})$ implies that

$$\mathbb{P}(p'_j(\mathbf{X}, \mathbf{y}) \leq u) \leq \mathbb{P}(p_j(\mathbf{X}, \mathbf{y}) \leq u) \leq u,$$

making p'_j also a valid p -value. The above discussion is summarized as the following theorem.

Theorem 2. *Let j be a null variable. For any screening rule S , the screened p -value $p'_j(\mathbf{X}, \mathbf{y})$ obtained from equation (1) is stochastically larger than uniform, i.e.,*

$$\mathbb{P}(p'_j(\mathbf{X}, \mathbf{y}) \leq u) \leq u \text{ for all } u \in [0, 1].$$

Thus, with the small computational overhead of a single well-chosen screening function, we can expect to dramatically cut the computation time of using the (d)CRT for variable selection. Note that the screening procedure increases the p -values relative to their unscreened counterparts, but it nevertheless has no impact on power as long as it does not screen away any non-null p -values that would have been rejected by a multiple testing procedure, which is far less-stringent and more

achievable than requiring the screening not to screen away *any* non-null p -values. In other words, imagine applying a Bonferroni correction (or the Benjamini–Hochberg procedure) to the screened p -values: there would only be a loss in power if the screening procedure failed to select a variable whose CRT p -value was less than α/p —however, any reasonable screening procedure will not fail to pick up such a strong signal. Indeed we found in our simulations that simple screenings were able to substantially decrease computation time without affecting the power.

3.2 Recycling computation for L_1 -regularized M -estimators

In some cases, we may want to compute p -values for all variables under consideration, even if only a small fraction of these are statistically significant. For instance, these may be needed for downstream analysis tasks like calibration assessment or meta-analysis. In such cases, we must look beyond the screening approach. In this section, we present a way of recycling computation for L_1 -regularized M -estimators including the lasso (recall Examples 1 and 2). This reduces the number of \mathcal{D}_y computations from p to $|\mathcal{A}|$, where \mathcal{A} is the active set of the lasso applied to (\mathbf{X}, \mathbf{y}) .

Let \mathcal{D}_y be the cross-validated lasso with strictly convex and differentiable loss function ℓ . Variable selection via the dCRT based on this distillation function requires computing

$$\widehat{\beta}(\mathbf{X}_{\bullet,-j}, \mathbf{y}; \lambda) := \arg \min_{\beta \in \mathbb{R}^{p-1}} \sum_{i=1}^n \ell(Y_i, X_{i,-j}\beta) + \lambda \|\beta\|_1 \quad (2)$$

for each $j = 1, \dots, p$, along a grid of regularization parameters. There is redundancy among these p lasso problems; they all differ from the the full lasso problem on (\mathbf{X}, \mathbf{y}) by just one variable. We may therefore expect that we can save computation by somehow recycling computation across these lasso problems. The next lemma suggests a means to this end:

Lemma 1. *Suppose the columns of \mathbf{X} are in general position and that the loss ℓ is differentiable and strictly convex. Then, for any $\lambda > 0$,*

$$\widehat{\beta}_j(\mathbf{X}, \mathbf{y}; \lambda) = 0 \implies \widehat{\beta}(\mathbf{X}_{\bullet,-j}, \mathbf{y}; \lambda) = \widehat{\beta}_{-j}(\mathbf{X}, \mathbf{y}; \lambda). \quad (3)$$

In words, Lemma 1 states that removing an inactive variable from the lasso does not change the fitted coefficient vector. This has important computational implications (potentially even outside the scope of this paper)—it suggests that we can avoid refitting the lasso (2) for most variables j , instead recycling the lasso fit on the full design matrix. Of course, the parameter λ is usually tuned via cross-validation, which introduces extra complications. However, we claim that if λ is chosen in an appropriate data-dependent way, then an analogous result will still hold.

To make this precise, consider a grid of regularization parameters

$$\lambda(1) > \lambda(2) > \dots > \lambda(G) > 0 \quad (4)$$

and a corresponding set of CV errors $\mathcal{E}_1, \dots, \mathcal{E}_G$. Define a rule \widehat{g} to select the penalty parameter λ based on CV errors $\mathcal{E}_1, \dots, \mathcal{E}_G$ to be *sequential* if these values are traversed in this order, and at some stopping time \widetilde{g} , the algorithm terminates and chooses $\lambda(\widehat{g})$ for some $\widehat{g} \leq \widetilde{g}$. For example, for any integer $\Delta \geq 1$, the following rule is sequential:

$$\widehat{g} \equiv \min\{g : \mathcal{E}_g \leq \min(\mathcal{E}_{g+1}, \dots, \mathcal{E}_{g+\Delta})\},$$

which is the first time along the regularization path that the CV error is smaller than the following Δ steps (the first ‘local minimum’ on the CV path, and the ‘sparsest’ of all such local minima). In this case the stopping time is $\widetilde{g} = \widehat{g} + \Delta$. The lasso with any sequential rule \widehat{g} has the property (3).

Theorem 3. Fix a grid of regularization parameters (4). Consider applying L_1 -regularized regression with loss ℓ on the whole data (\mathbf{X}, \mathbf{y}) , with λ selected by K -fold cross-validation and a sequential stopping rule \hat{g} . Let $\hat{g}(\mathbf{X}, \mathbf{y})$ and $\tilde{g}(\mathbf{X}, \mathbf{y})$ be the resulting grid point and stopping time, respectively. Letting $\{1, \dots, n\} = D_1 \cup \dots \cup D_K$ denote the split of the data into folds, define the active set

$$\mathcal{A} = \{j \in \{1, \dots, p\} : \hat{\beta}_j(\mathbf{X}, \mathbf{y}; \lambda(\hat{g}(\mathbf{X}, \mathbf{y}))) \neq 0 \text{ or } \hat{\beta}_j(\mathbf{X}_{-D_k, \bullet}, \mathbf{y}_{-D_k}; \lambda(g)) \neq 0 \text{ for some } k, g \leq \tilde{g}(\mathbf{X}, \mathbf{y})\}. \quad (5)$$

If the loss ℓ is differentiable and strictly convex, and the columns of \mathbf{X} and $\mathbf{X}_{-D_k, \bullet}$ are in general position for each k , then excluding non-active variables j does not alter the fitted coefficients:

$$\text{for each } j \notin \mathcal{A}, \hat{g}(\mathbf{X}_{\bullet, -j}, \mathbf{y}) = \hat{g}(\mathbf{X}, \mathbf{y}) \text{ and } \hat{\beta}_j(\mathbf{X}_{\bullet, -j}, \mathbf{y}; \lambda(\hat{g}(\mathbf{X}_{\bullet, -j}, \mathbf{y}))) = \hat{\beta}_j(\mathbf{X}, \mathbf{y}; \lambda(\hat{g}(\mathbf{X}, \mathbf{y}))). \quad (6)$$

Proposition 3 states that for each variable j not in the active set, we need not re-run the lasso holding out variable j ; we can instead fit the full lasso once and then read off the coefficient vector. This computational shortcut, summarized in Algorithm A2, reduces the number of lasso applications required by the dCRT from p to $|\mathcal{A}|$. Depending on the sparsity of the problem, this reduction can save several orders of magnitude of computation. It is known that at most, the lasso solution has $\min(p, n)$ nonzero entries (Tibshirani, 2013), though in most cases it is much sparser.

4 Simulations

In the interest of space we defer the details of our myriad simulations to the appendix and present here a detailed summary of the takeaways of those simulations, directly linking each takeaway to the figure and section of the appendix with the corresponding simulation(s) supporting it. The main focus of our simulations is examining the performance of the dCRT through the d_0 CRT and d_1 CRT given by Examples 1 and 2, respectively. Except where explicitly stated otherwise, we apply them in a resampling-free manner per Section 2.4 and, when simulating a variable selection task, with screening (using the cross-validated lasso for selection) per Section 3.1. For variable selection simulations, we take each of the p -value methods (CRT, dCRT, HRT) and apply the Benjamini–Hochberg procedure when targeting FDR control and the Bonferroni correction when targeting FWER control.¹

Distillation dramatically reduces CRT computation while retaining comparable power.

In simulations with linear and logistic regression models, a range of signal amplitudes, and $n = p = 300$ (the data size was deliberately limited to accommodate the computational burden of the original CRT), both the d_0 CRT and d_1 CRT conferred a computational savings of approximately 500 times over the original CRT (Table A1) while maintaining essentially the same power (Figures A2, A3). See Appendix D.2 for details.

The dCRT is more powerful than the HRT. In both the aforementioned $n = p = 300$ simulations and a larger simulation with $n = p = 800$, the dCRT computation times were mostly within an order of magnitude of the HRT (Tables A1 and A2). But across settings that included a range of n up to 1400, a range of p up to 3200, a range of signal magnitudes, a range of sparsities, a range of covariance structures for X , and a range of models for $Y | X$, both dCRT methods

¹Source code for running the dCRT and reproducing our results can be found along with example scripts for illustration at <https://github.com/moleibobliu/Distillation-CRT>.

had consistently and substantially higher power than the HRT (up to about 50 percentage points higher); see Figures A2, A3, A4, A5, A6, A7, A8. See Appendices D.2 and D.3 for details.

When controlling FDR, the relative performance of dCRT and knockoffs varies across simulation settings. The relationship between the power of dCRT and that of knockoffs is less clear, and different simulation settings lead to different relative performances. The dCRT methods tend to have higher power than knockoffs when signal variables are correlated with one another and lower power than knockoffs when the signal variables are nearly uncorrelated. In very sparse settings, dCRT still has power, while knockoffs does not (due to its reliance on the Selective SeqStep+ procedure (Barber and Candès, 2015)). In such regimes, the FWER may be more appropriate, and the dCRT can be used to control this error rate as well. See Figures A2, A3, A4, A5, A6, A7, A8. The dCRT is more computationally expensive than knockoffs, but usually within an order of magnitude (Tables A1 and A2). See Appendices D.2 and D.3 for details.

The d₁CRT is stable to the choice of k and has slightly less power than the d₀CRT in additive models but can have substantially higher power in the presence of interactions. In a simulation with an additive model, the power of the d₁CRT was identical as k ranged from 2–22 (the default value of $k = 2 \log(p)$ would have been 13), while in a model with five true interactions, the power only varied from about 50% to about 40% over the same range of k (Figure A11). Throughout all our simulations in additive models we found the d₀CRT to be slightly but consistently more powerful than the d₁CRT (e.g., Figures A2, A3, A4, A5, A6, A7, A8, A13, A14), but in the presence of interactions obeying the hierarchy principle discussed in Section 2.3.2, we found that the d₁CRT could be quite a bit more powerful (up to about 25 percentage points) than the d₀CRT (Figure A10). See Appendices D.5 and D.6 for details.

The dCRT can leverage nonparametric machine learning algorithms for substantial power gains in highly-nonlinear models. In a simulation in which X 's relationship with Y was highly-nonlinear and interacted with five Z_j 's, our default (lasso-based) d₁CRT had somewhat higher power than d₀CRT (as much as about 20 percentage points), but a different, random-forest-based d₁CRT had far higher power than the lasso-based d₁CRT (as much as about 50 percentage points) (Figure A12). See Appendix D.7 for details.

The dCRT is quite robust to misspecification of X 's distribution. When the distribution of $X | Z$ is Poisson even with a very small mean parameter (making it highly discrete and heavily skewed) but approximated by a Gaussian with matching mean and variance, both the d₀CRT and d₁CRT maintain Type-I error control and high power (Figure A13). Furthermore, when the covariates are jointly Gaussian but their covariance matrix is estimated in-sample, the Type-I error of both dCRT methods does not inflate much above the nominal level even when a quite poor estimator is used (Figure A14). See Appendix D.8 for details.

The resampling-free versions of the dCRT are faster and just as powerful as the non-resampling-free dCRT except when $X | Z$ is highly discrete. The resampling-free modification sped up the d₀CRT by 2.5 times in an $n = p = 800$ simulation and sped up the d₁CRT by 11 times in an $n = p = 800$ simulation, even after applying screening (Table A3). When $X | Z$ is Gaussian, changing the form of the test statistics of the d₀CRT and d₁CRT as proposed in paragraphs 2 and 4, respectively, of Section 2.4 had a negligible effect on their power (Figure A16). When $X | Z$ is non-Gaussian and must be transformed to Gaussian as described in paragraph 3 of

Section 2.4, we found essentially no power loss for the resampling-free d_0 CRT and d_1 CRT relative to their non-resampling-free counterparts when $X | Z$ was Gamma-distributed (with shape = 3 and rate = 0.5, so that skew > 1 and excess kurtosis = 2), while there was substantial power loss (up to about 40 percentage points) when $X | Z$ was binary and hence required substantial exogenous randomization to be transformed to Gaussian, though the resampling-free dCRTs were still substantially more powerful (up to about 10 percentage points) than the HRT (Figure A17). See Appendix D.9 for details.

Screening makes the dCRT faster without affecting its power. In a simulation with $n = p = 800$, screening reduced the computation time by a factor of about 5 for both d_0 CRT and d_1 CRT (Table A4) without perceptibly hurting power (Figure A18). See Appendix D.10 for details.

5 Identifying biomarkers for breast cancer

As a final demonstration of the effectiveness of the dCRT, we apply it to the data set from Curtis et al. (2012), consisting of $n = 1,396$ staged oestrogen-receptor-positive cases of breast cancer, each with expression level (mRNA) and copy number aberration (CNA) measured for $p = 164$ genes, which were studied in Pereira et al. (2016). Our goal is to find genes on which cancer stage depends, conditional on the remaining genes and all CNAs, while controlling either the FDR or FWER at level 0.1. Discovering such biomarkers for cancer can reveal new pathways and mechanisms for cancer progression; see Shen et al. (2019) for a recent application of model-X knockoffs to the same end.

After log-transforming the gene expressions, we adjust to them using the CNA data with linear model as in Solvang et al. (2011); Lahti et al. (2012); Leday et al. (2013) and modeled the processed gene expressions jointly as multivariate Gaussian similar to Shen et al. (2019). We applied the d_0 CRT, the d_1 CRT, the original lasso-based CRT, the HRT, and model-X knockoffs and compared the results. See Appendix E for details of the data pre-processing, covariate-modeling, and method implementations. Table 1 contains the numbers of discoveries and runtimes (in R) for all the methods, showing that the dCRTs are quite fast and make the most discoveries on this data set. In particular, the original CRT takes over 5 hours to run while the dCRTs take under a minute, and the HRT and knockoffs make three and zero discoveries respectively for FDR control, and HRT makes three discoveries for FWER control. Knockoffs’ lack of power is due to the sparsity of discoverable genes.

Method	Discoveries (FDR)	Discoveries (FWER)	Time (minutes)
d_0 CRT	5	3	0.5
d_1 CRT	5	4	0.5
CRT	4	2	333.4
HRT	3	3	1.1
Knockoffs	0	N/A	0.1

Table 1: Numbers of discoveries and computation times (in R) of different methods, with FDR and FWER control, in the breast cancer application. The dCRT approaches are more powerful than the competitors, even the usual full CRT. Note that our use of the resampling-free version of the dCRT makes it faster than the HRT in this case.

When used to control the FDR, it turns out that all five genes discovered by the dCRT (*FBXW7*, *MAP3K13*, *HRAS*, *GPS2*, and *RUNX1*; see Appendix A5 for their corresponding p -values) have

been linked in independent research to cancer, suggesting the dCRT makes promising discoveries. In particular, *FBXW7* encodes a member of the F-box protein family and its mutations are detected in ovarian and breast cancer cell lines (Liu et al., 2019; Kirzinger et al., 2019); *MAP3K13* belongs to the serine/threonine protein kinase family acting as a regulator for cancer (Han et al., 2016); *HRAS* belongs to the RAS oncogene family which is related to the transforming of genes of mammalian sarcoma retroviruses, and defects in this gene have been implicated in a variety of cancers (Geyer et al., 2018); over-expression of *GPS2* in mammalian cells may suppress signals mediated by RAS/MAPK and interfere with JNK activity, all of which are cancer-related (Jarmalavicius et al., 2010; Huang et al., 2016); *RUNX1* has been found to activate certain signaling pathways that promote tumor metastasis (Li et al., 2019).

6 Discussion

The HRT provided the first indication that a variant of the CRT could be computationally tractable, albeit at the cost of statistical performance. In this paper, we demonstrate that leaving out *variables* instead of *samples* creates a procedure that is not quite as fast (though still a tiny fraction of the CRT’s computational cost) but much more powerful. This brings the dCRT into the realm of fast and powerful model-X methods, where knockoffs is currently the methodology of choice. Knockoffs and dCRT have complementary strengths and weaknesses, which we discuss briefly below.

Model-X knockoffs addresses the variable selection problem, targeting FDR control. It is very computationally efficient, requiring just one high-dimensional model fit. Furthermore, our simulations confirm that knockoffs is quite powerful in many simulation settings. These advantages have led to the successful application of knockoffs to genome-wide association studies (GWAS) (Sesia et al., 2019, 2020). By comparison, the dCRT still requires several high-dimensional model fits and is therefore more computationally costly. On the other hand, dCRT computation benefits from being embarrassingly parallelizable, so modern parallel computing resources can greatly reduce its runtime. As far as power goes, the relative performance of the two methods varies with simulation setting (see Section 4 and supplementary Section D); neither procedure uniformly dominates the other (when controlling the FDR).

Aside from these considerations, the dCRT provides a few important advantages over knockoffs. The first is that, unlike knockoffs, the dCRT provides p -values (arbitrarily fine-grained and essentially exact) for each conditional independence hypothesis. In addition to providing an interpretable measure of significance, this decoupling of statistical significance quantification from downstream analyses such as multiple testing brings great versatility. Indeed, dCRT p -values can be used for single hypothesis testing, multiple hypothesis testing with a variety of error rates, and any number of other tasks that take p -values as input. While the knockoffs framework has gradually been extended to handle analysis tasks beyond FDR control (e.g. k -FWER control by Janson and Su (2016), and simultaneous FDP control by Katsevich and Ramdas (2020a)), such extensions require custom solutions and some are in fact impossible (such as single testing or FWER control). Another advantage of the dCRT is that it has little or no variability across runs. On the other hand, knockoffs is a randomized procedure; this randomization can lead to variability in the performance of the procedure on a given data set (see Section C in the supplement and Figure 4 of Sesia et al. (2019)).

The dCRT is therefore a useful addition to the model-X methodology toolbox. Much work still remains to refine this new tool for better power and even faster computation. Indeed, many degrees of freedom in the construction of the dCRT test statistic remain to be explored. For example, should the statistic be based on the fitted coefficient of a variable or on the loss function? What is the

best way to test groups of variables? The recent theoretical exploration of the CRT (Katsevich and Ramdas, 2020b) may help guide the search for powerful test statistics. Another open question is whether there are efficient resampling-free dCRT variants for highly discrete covariates. Finally, the dependence structure of (d)CRT p -values is an important subject for further exploration. We may not always be able to plug-and-play (d)CRT p -values in multiple testing procedures, since their dependency structure is currently unknown. In a related development, Bates et al. (2020) recently proposed a clever method of generating independent HRT p -values for groups of linearly-structured covariates.

Despite these open questions, our initial demonstrations of the dCRT on simulated and real data are quite promising. We are therefore optimistic about the prospects of the dCRT for fruitful practical applications, and look forward to continued improvements in the computational and statistical efficiency of model-X methodology.

Acknowledgements

We would like to thank Siyuan Ma, Wenshuo Wang, Dae Woong Ham, and Lu Zhang for helpful discussions and feedback on the paper. This work used the Extreme Science and Engineering Discovery Environment (XSEDE) Towns et al. (2014), which is supported by National Science Foundation grant number ACI-1548562. Specifically, it used the Bridges system Nystrom et al. (2015), which is supported by NSF award number ACI-1445606, at the Pittsburgh Supercomputing Center (PSC).

References

- Barber, R. F. and Candès, E. J. (2015). Controlling the false discovery rate via knockoffs. *The Annals of Statistics*, 43(5):2055–2085.
- Bates, S., Sesia, M., Sabatti, C., and Candès, E. (2020). Causal inference in genetic trio studies. *arXiv preprint arXiv:2002.09644*.
- Bellot, A. and van der Schaar, M. (2019). Conditional independence testing using generative adversarial networks. In *Advances in Neural Information Processing Systems*, pages 2199–2208.
- Benjamini, Y. and Hochberg, Y. (1995). Controlling the false discovery rate: a practical and powerful approach to multiple testing. *Journal of the Royal Statistical Society: Series B*, 57(1):289–300.
- Benjamini, Y. and Yekutieli, D. (2001). The control of the false discovery rate in multiple testing under dependency. *The Annals of Statistics*, 29(4):1165–1188.
- Berrett, T. B., Wang, Y., Barber, R. F., and Samworth, R. J. (2019). The conditional permutation test for independence while controlling for confounders. *Journal of the Royal Statistical Society: Series B*.
- Bien, J., Taylor, J., and Tibshirani, R. (2013). A lasso for hierarchical interactions. *Annals of Statistics*, 41(3):1111.
- Candès, E., Fan, Y., Janson, L., and Lv, J. (2018). Panning for gold: model-X knockoffs for high dimensional controlled variable selection. *Journal of the Royal Statistical Society: Series B*, 80(3):551–577.

- Chernozhukov, V., Chetverikov, D., Demirer, M., Duflo, E., Hansen, C., and Newey, W. K. (2016). Double machine learning for treatment and causal parameters. Technical report, Cemmap working paper.
- Chipman, H. (1996). Bayesian variable selection with related predictors. *Canadian Journal of Statistics*, 24(1):17–36.
- Cox, D. R. (1984). Interaction. *International Statistical Review*, pages 1–24.
- Curtis, C., Shah, S. P., Chin, S.-F., Turashvili, G., Rueda, O. M., Dunning, M. J., Speed, D., Lynch, A. G., Samarajiwa, S., Yuan, Y., et al. (2012). The genomic and transcriptomic architecture of 2,000 breast tumours reveals novel subgroups. *Nature*, 486(7403):346–352.
- Davies, R. B. (1980). Algorithm as 155: The distribution of a linear combination of χ^2 random variables. *Journal of the Royal Statistical Society: Series C*, 29(3):323–333.
- Duchesne, P. and De Micheaux, P. L. (2010). Computing the distribution of quadratic forms: Further comparisons between the Liu–Tang–Zhang approximation and exact methods. *Computational Statistics & Data Analysis*, 54(4):858–862.
- Friedman, J., Hastie, T., and Tibshirani, R. (2008). Sparse inverse covariance estimation with the graphical lasso. *Biostatistics*, 9(3):432–441.
- Geyer, F. C., Li, A., Papanastasiou, A. D., Smith, A., Selenica, P., Burke, K. A., Edelweiss, M., Wen, H. C., Piscuoglio, S., and Schultheis, A. M. (2018). Recurrent hotspot mutations in HRAS-Q61 and PI3K-AKT pathway genes as drivers of breast adenomyoepitheliomas. *Nature Communications*, 9(1):1–16.
- Hamada, M. and Wu, C. J. (1992). Analysis of designed experiments with complex aliasing. *Journal of Quality Technology*, 24(3):130–137.
- Han, H., Chen, Y., Cheng, L., Prochownik, E. V., and Li, Y. (2016). microRNA-206 impairs c-Myc-driven cancer in a synthetic lethal manner by directly inhibiting MAP3K13. *Oncotarget*, 7(13):16409.
- Huang, J., Ma, S., and Zhang, C.-H. (2008). Adaptive lasso for sparse high-dimensional regression models. *Statistica Sinica*, pages 1603–1618.
- Huang, X., Xiao, F., Wang, S., Yin, R., Lu, C., Li, Q., Liu, N., Wang, L., and Li, P. (2016). G protein pathway suppressor 2 (GPS2) acts as a tumor suppressor in liposarcoma. *Tumor Biology*, 37(10):13333–13343.
- Imhof, J. P. (1961). Computing the distribution of quadratic forms in normal variables. *Biometrika*, 48(3/4):419–426.
- Janson, L. and Su, W. (2016). Familywise error rate control via knockoffs. *Electronic Journal of Statistics*, 10:960–975.
- Jarmalavicius, S., Trefzer, U., and Walden, P. (2010). Differential arginine methylation of the G-protein pathway suppressor GPS-2 recognized by tumor-specific T-cells in melanoma. *The FASEB Journal*, 24(3):937–946.
- Katsevich, E. and Ramdas, A. (2020a). Simultaneous high-probability bounds on the false discovery proportion in structured, regression, and online settings. *The Annals of Statistics*, to appear.

- Katsevich, E. and Ramdas, A. (2020b). A theoretical treatment of conditional independence testing under model-X. *arXiv preprint arXiv:2005.05506*.
- Kirzinger, M. W., Vizeacoumar, F. S., Haave, B., Gonzalez Lopez, C., Bonham, K., Kusalik, A., and Vizeacoumar, F. J. (2019). Humanized yeast genetic interaction mapping predicts synthetic lethal interactions of FBXW7 in breast cancer. *BMC medical genomics*, 12(1):112.
- Lahti, L., Schäfer, M., Klein, H. U., Bicciato, S., and Dugas, M. (2012). Cancer gene prioritization by integrative analysis of mRNA expression and dna copy number data: a comparative review. *Briefings in Bioinformatics*, 14(1):27–35.
- Leday, G. G., van der Vaart, A. W., van Wieringen, W. N., and van de Wiel, M. A. (2013). Modeling association between DNA copy number and gene expression with constrained piecewise linear regression splines. *The Annals of Applied Statistics*, pages 823–845.
- Li, Q., Lai, Q., He, C., Fang, Y., Yan, Q., Zhang, Y., Wang, X., Gu, C., Wang, Y., Ye, L., Han, L., Lin, X., Chen, J., Cai, J., Li, A., and Liu, S. (2019). RUNX1 promotes tumour metastasis by activating the Wnt/ β -catenin signalling pathway and EMT in colorectal cancer. *Journal of Experimental & Clinical Cancer Research*, 38(1):334.
- Liu, F., Zou, Y., Wang, F., Yang, B., Zhang, Z., Luo, Y., Liang, M., Zhou, J., and Huang, O. (2019). FBXW7 mutations promote cell proliferation, migration, and invasion in cervical cancer. *Genetic testing and molecular biomarkers*, 23(6):409–417.
- Liu, H., Tang, Y., and Zhang, H. H. (2009). A new chi-square approximation to the distribution of non-negative definite quadratic forms in non-central normal variables. *Computational Statistics & Data Analysis*, 53(4):853–856.
- Nelder, J. (1977). A reformulation of linear models. *Journal of the Royal Statistical Society: Series A*, 140(1):48–63.
- Nystrom, N. A., Levine, M. J., Roskies, R. Z., and Scott, J. R. (2015). Bridges: A Uniquely Flexible HPC Resource for New Communities and Data Analytics. In *Proceedings of the 2015 XSEDE Conference: Scientific Advancements Enabled by Enhanced Cyberinfrastructure*, XSEDE '15, pages 30:1—30:8, New York, NY, USA. ACM.
- Peixoto, J. L. (1987). Hierarchical variable selection in polynomial regression models. *The American Statistician*, 41(4):311–313.
- Pereira, B., Chin, S.-F., Rueda, O. M., Vollan, H.-K. M., Provenzano, E., Bardwell, H. A., Pugh, M., Jones, L., Russell, R., Sammut, S.-J., Tsui, D. W. Y., Liu, B., Dawson, S.-J., Abraham, J., Northen, H., Peden, J. F., Mukherjee, A., Turashvili, G., Green, A. R., McKinney, S., Oloumi, A., Shah, S., Rosenfeld, N., Murphy, L., Bentley, D. R., Ellis, I. O., Purushotham, A., Pinder, S. E., Brresen-Dale, A.-L., Earl, H. M., Pharoah, P. D., Ross, M. T., Aparicio, S., and Caldas, C. (2016). The somatic mutation profiles of 2,433 breast cancers refine their genomic and transcriptomic landscapes. *Nature communications*, 7:11479.
- Sesia, M., Katsevich, E., Bates, S., Candès, E., and Sabatti, C. (2020). Multi-resolution localization of causal variants across the genome. *Nature Communications*, 11:1093.
- Sesia, M., Sabatti, C., and Candès, E. J. (2019). Gene hunting with hidden Markov model knockoffs. *Biometrika*, 106(1):1–18.

- Shah, R. D. and Peters, J. (2018). The hardness of conditional independence testing and the generalised covariance measure. *Annals of Statistics, to appear*.
- Shen, A., Fu, H., He, K., and Jiang, H. (2019). False discovery rate control in cancer biomarker selection using knockoffs. *Cancers*, 11(6):744.
- Solvang, H. K., Lingjærde, O. C., Frigessi, A., Børresen Dale, A. L., and Kristensen, V. N. (2011). Linear and non-linear dependencies between copy number aberrations and mRNA expression reveal distinct molecular pathways in breast cancer. *BMC bioinformatics*, 12(1):197.
- Tansey, W., Veitch, V., Zhang, H., Rabadan, R., and Blei, D. M. (2018). The holdout randomization test: Principled and easy black box feature selection. *arXiv preprint arXiv:1811.00645*.
- Tibshirani, R. (1996). Regression shrinkage and selection via the lasso. *Journal of the Royal Statistical Society: Series B*, 58(1):267–288.
- Tibshirani, R. J. (2013). The lasso problem and uniqueness. *Electronic Journal of Statistics*, 7:1456–1490.
- Towns, J., Cockerill, T., Dahan, M., Foster, I., Gauthier, K., Grimshaw, A., Hazlewood, V., Lathrop, S., Lifka, D., Peterson, G. D., Roskies, R., Scott, J., and Wilkins-Diehr, N. (2014). XSEDE: Accelerating Scientific Discovery. *Computing in Science & Engineering*, 16(05):62–74.
- Zou, H. (2006). The adaptive lasso and its oracle properties. *Journal of the American Statistical Association*, 101(476):1418–1429.
- Zou, H. and Hastie, T. (2005). Regularization and variable selection via the elastic net. *Journal of the Royal Statistical Society: Series B*, 67(2):301–320.

A Resampling-free dCRT

A.1 Resampling-free lasso-based d₁CRT

In this section, we describe the resampling-free version of the lasso-based d₁CRT of Example 2 for gaussian X , in analog to the resampling-free d₀CRT detailed in Section 2.4. We follow the notation of Example 2 and for any $\mathbf{a} = (a_1, \dots, a_n)^\top \in \mathbb{R}^n$, let $\text{diag}(\mathbf{a})$ denote the diagonal matrix with its (i, i) -th entry being a_i for $i = 1, 2, \dots, n$. Then in Example 2,

$$\begin{aligned} \hat{\beta}_x &= \left[(\mathbf{1}, \mathbf{Z}_{\bullet, \text{top}(k)})^\top \text{diag}^2(\boldsymbol{\epsilon}_x) (\mathbf{1}, \mathbf{Z}_{\bullet, \text{top}(k)}) \right]^{-1} (\mathbf{1}, \mathbf{Z}_{\bullet, \text{top}(k)})^\top \text{diag}(\boldsymbol{\epsilon}_x) (\mathbf{y} - \mathbf{d}_y) \\ &= \hat{\mathbb{H}}^{-1} (\mathbf{1}, \mathbf{Z}_{\bullet, \text{top}(k)})^\top \text{diag}(\mathbf{y} - \mathbf{d}_y) \boldsymbol{\epsilon}_x, \end{aligned}$$

where $\hat{\mathbb{H}} = (\mathbf{1}, \mathbf{Z}_{\bullet, \text{top}(k)})^\top \text{diag}^2(\boldsymbol{\epsilon}_x) (\mathbf{1}, \mathbf{Z}_{\bullet, \text{top}(k)})$ and $\boldsymbol{\epsilon}_x = \mathbf{x} - \mathbf{d}_x$. And the test statistics

$$T(\mathbf{y}, \mathbf{x}, \mathbf{d}_y, \mathbf{d}_x) = \hat{\beta}_{x,1}^2 + \frac{1}{k} \sum_{j=2}^{k+1} \hat{\beta}_{x,j}^2 = \|\hat{\mathbb{H}}^{-1} \tilde{\mathbf{Z}}_{\bullet, \text{top}(k)} \boldsymbol{\epsilon}_x\|_2^2$$

where $\tilde{\mathbf{Z}}_{\bullet, \text{top}(k)} = (\mathbf{1}, k^{-1/2} \mathbf{Z}_{\bullet, \text{top}(k)})^\top \text{diag}(\mathbf{y} - \mathbf{d}_y)$. In analog to the resampling-free d₀CRT introduced in Section 2.4, we replace $\hat{\mathbb{H}}$ with its conditional expectation given (\mathbf{y}, \mathbf{Z}) , i.e., $\mathbb{H} = \sigma_x^2 (\mathbf{1}, \mathbf{Z}_{\bullet, \text{top}(k)})^\top (\mathbf{1}, \mathbf{Z}_{\bullet, \text{top}(k)})$ with σ_x^2 being the conditional variance of X given Z . Then the test statistics of the resampling-free version of d₁CRT can be constructed as $\|\mathbb{H}^{-1} \tilde{\mathbf{Z}}_{\bullet, \text{top}(k)} \boldsymbol{\epsilon}_x\|_2^2$. Conditional on (\mathbf{y}, \mathbf{Z}) , it is a quadratic form of the gaussian vector $\boldsymbol{\epsilon}_x$ under the null. Accurate and efficient computational methods have been proposed to handle such problems (see, e.g., Imhof (1961); Davies (1980); Liu et al. (2009)). We use the method proposed by Imhof (1961) and realized by R package `CompQuadForm` (Duchesne and De Micheaux, 2010) to compute the p -value of $\|\mathbb{H}^{-1} \tilde{\mathbf{Z}}_{\bullet, \text{top}(k)} \boldsymbol{\epsilon}_x\|_2^2$.

A.2 Resampling-free dCRT with non-Gaussian X

Let $\Phi(\cdot)$ denote the cumulative distribution function (CDF) of the standard normal distribution and denote by $\sigma_i^2 = \text{Var}(X_i | Z_i)$. In Algorithm A1, we describe how to transform non-Gaussian X to be Gaussian with the same conditional variance, so that the resampling-free dCRT (for certain statistics) can be applied. Lemma A1 establishes the properties that make \mathbf{u} a good Gaussian

Algorithm A1 Gaussian transformation.

if X is continuous with conditional CDF $F(x | Z)$, **then**

For $i = 1, 2, \dots, n$: let $U_i = \sigma_i \Phi^{-1}(F(X_i | Z_i))$.

end if

if X is discrete and supported on $\mathcal{X} = \{a_k : k \in K\}$ where $K \subseteq \mathbb{N}$ is some set of indices, $a_{k_1} < a_{k_2}$ for all $k_1 < k_2$ and $\mathbb{P}(X_i = a_k | Z_i) \neq 0$ for all $k \in K$, **then**

For $i = 1, 2, \dots, n$: if $X_i = a_k$, draw V_i uniformly from $[\mathbb{P}(X_i < a_k | Z_i), \mathbb{P}(X_i \leq a_k | Z_i)]$ and let $U_i = \sigma_i \Phi^{-1}(V_i)$.

end if

Output $\mathbf{u} = (U_1, U_2, \dots, U_n)^\top$.

stand-in for $\mathbf{x} - \mathbf{d}_x$, so that it can be used in a test statistic T in the same way as $\mathbf{x} - \mathbf{d}_x$ while being amenable to the resampling-free speedup.

Lemma A1. *The U_i output by Algorithm A1 are (i) monotonically increasing in X_i , (ii) distributed as $\mathcal{N}(0, \sigma_i^2)$ given Z_i , and (iii) independent from Z_i .*

Proof. For (i), when X_i is continuous, we note that both $\Phi(x)$ and $F(x | Z_i)$ are increasing and this implies U_i is unique and monotonically increasing with X_i . When X_i is discrete, noting that the range of V_i does not intersect as X_i takes different values and the range of V_i is increasing with X_i , we again have that U_i is monotonically increasing with X_i .

For (ii), when X_i is continuous, let $V_i = F(X_i | Z_i)$ and when X_i is discrete, let V_i be defined as in Algorithm A1. Since V_i is uniformly distributed on $[0, 1]$ conditional on Z_i , we have that for any $u \in \mathbb{R}$,

$$\mathbb{P}(U_i \leq u | Z_i) = \mathbb{P}(\Phi(U_i/\sigma_i) \leq \Phi(u/\sigma_i) | Z_i)$$

which indicates that $\mathbb{P}(U_i/\sigma_i \leq v | Z_i) = \Phi(v)$ and $U_i \sim \mathcal{N}(0, \sigma_i^2)$. Also, we have $\mathbb{P}(U_i/\sigma_i \leq v) = \Phi(v) = \mathbb{P}(U_i/\sigma_i \leq v | Z_i)$ for all $v \in \mathbb{R}$, which indicates that $U_i/\sigma_i \perp Z_i$. \square

B Recycling computation for lasso-based distillation

Here, prove Lemma 1 and Theorem 3 from Section 3.2. These lead to Algorithm A2 below, which we call L1ME dCRT (pronounced “lime”, stands for L_1 -regularized M-estimator).

Algorithm A2 dCRT for L_1 -regularized M-estimators (L1ME dCRT)

Input: \mathbf{X}, \mathbf{y} , sequence $\lambda(1) > \dots > \lambda(G) > 0$, loss ℓ , sequential rule \hat{g}

Fit a cross-validated lasso on (\mathbf{X}, \mathbf{y}) to obtain $\hat{\beta}(\mathbf{X}, \mathbf{y}; \lambda(\hat{g}(\mathbf{X}, \mathbf{y})))$, and record the active set \mathcal{A} as defined in (5).

for $j \in \mathcal{A}$ **do**

Refit the lasso on $(\mathbf{X}_{\bullet, -j}, \mathbf{y})$ to obtain $\hat{\beta}_{-j} \equiv \hat{\beta}(\mathbf{X}_{\bullet, -j}, \mathbf{y}; \lambda(\hat{g}(\mathbf{X}_{\bullet, -j}, \mathbf{y})))$.

end for

for $j \notin \mathcal{A}$ **do**

Set $\hat{\beta}_{-j} = \hat{\beta}_{-j}(\mathbf{X}, \mathbf{y}; \lambda(\hat{g}(\mathbf{X}, \mathbf{y})))$.

end for

For each j , let $d_{\mathbf{y}, j} = \mathbf{X}_{\bullet, -j} \hat{\beta}_{-j}$

Output: Distillations $d_{\mathbf{y}, j}$ for each variable j .

Proof of Lemma 1. Since $\hat{\beta}(\mathbf{X}, \mathbf{y}; \lambda)$ is a minimizer of the convex objective

$$\sum_{i=1}^n \ell(\mathbf{y}_i, \mathbf{X}_{i, \bullet} \beta) + \lambda \|\beta\|_1, \quad (7)$$

0 must belong to its subgradient at this point. This means that there exists an $\hat{\mathbf{s}} \in \mathbb{R}^p$ such that

$$\sum_{i=1}^n \mathbf{X}_{i, j'} \dot{\ell}(\mathbf{y}_i, \mathbf{X}_{i, \bullet} \hat{\beta}(\mathbf{X}, \mathbf{y}; \lambda)) + \lambda \cdot \hat{\mathbf{s}}_{j'} = 0 \quad \text{for all } j' = 1, \dots, p, \quad (8)$$

where $\hat{\mathbf{s}}_{j'} = \text{sign}(\hat{\beta}_{j'}(\mathbf{X}, \mathbf{y}; \lambda))$ if $\hat{\beta}_{j'}(\mathbf{X}, \mathbf{y}; \lambda) \neq 0$ and $\hat{\mathbf{s}}_{j'} \in [-1, 1]$ otherwise. If $\hat{\beta}_j(\mathbf{X}, \mathbf{y}; \lambda) = 0$, then we have

$$\mathbf{X}_{i, -j} \hat{\beta}_{-j}(\mathbf{X}, \mathbf{y}; \lambda) = \mathbf{X}_{i, \bullet} \hat{\beta}(\mathbf{X}, \mathbf{y}; \lambda) \quad \text{for every } i = 1, \dots, n,$$

which together with equation (8) implies that

$$\text{for all } j' \neq j, \quad \sum_{i=1}^n \mathbf{X}_{i,j'} \dot{\ell}(\mathbf{y}_i, \mathbf{X}_{i,-j} \widehat{\beta}_{-j}(\mathbf{X}, \mathbf{y}; \lambda)) + \lambda \cdot s_{j'} = 0.$$

Therefore, $\widehat{\beta}_{-j}(\mathbf{X}, \mathbf{y}; \lambda)$ satisfies the first-order optimality condition in the convex problem (2), so it must be a minimizer. Given the assumed general position of the columns of \mathbf{X} and the assumptions on ℓ , the minimizer of the problem (2) is unique (Tibshirani, 2013). Therefore, $\widehat{\beta}(\mathbf{X}_{\bullet,-j}, \mathbf{y}; \lambda) = \widehat{\beta}_{-j}(\mathbf{X}, \mathbf{y}; \lambda)$, as desired. \square

Proof of Theorem 3. Fix $j \notin \mathcal{A}$. For this variable, $\widehat{\beta}_j(\mathbf{X}_{-D_k, \bullet}, \mathbf{y}_{-D_k}; \lambda(g)) = 0$ for each fold k and for all $g \leq \widetilde{g}(\mathbf{X}, \mathbf{y})$. By Lemma 1 applied to $(\mathbf{X}_{-D_k, \bullet}, \mathbf{y}_{-D_k})$, it follows that

$$\widehat{\beta}(\mathbf{X}_{-D_k, -j}, \mathbf{y}_{-D_k}; \lambda(g)) = \widehat{\beta}_{-j}(\mathbf{X}_{-D_k, \bullet}, \mathbf{y}_{-D_k}; \lambda(g)) \quad \text{for each fold } k \text{ and all } g \leq \widetilde{g}(\mathbf{X}, \mathbf{y}).$$

Therefore, the lasso cross-validation errors for (\mathbf{X}, \mathbf{y}) and $(\mathbf{X}_{\bullet,-j}, \mathbf{y})$ coincide for each $g \leq \widetilde{g}(\mathbf{X}, \mathbf{y})$:

$$\mathcal{E}_{-j,g} = \sum_{i=1}^n \ell(\mathbf{y}_i, \mathbf{X}_{i,-j} \widehat{\beta}(\mathbf{X}_{-D_k, -j}, \mathbf{y}_{-D_k}; \lambda(g))) = \sum_{i=1}^n \ell(\mathbf{y}_i, \mathbf{X}_{i,\bullet} \widehat{\beta}(\mathbf{X}_{-D_k, \bullet}, \mathbf{y}_{-D_k}; \lambda(g))) = \mathcal{E}_g.$$

Because the rule to choose λ is sequential, we conclude that $\widetilde{g}(\mathbf{X}_{\bullet,-j}, \mathbf{y}) = \widetilde{g}(\mathbf{X}, \mathbf{y})$ and also $\widehat{g}(\mathbf{X}_{\bullet,-j}, \mathbf{y}) = \widehat{g}(\mathbf{X}, \mathbf{y})$. The conclusion (6) now follows from another application of Lemma 1, this time with the full data (\mathbf{X}, \mathbf{y}) and the regularization parameter $\lambda(\widehat{g}(\mathbf{X}_{\bullet,-j}, \mathbf{y})) = \lambda(\widehat{g}(\mathbf{X}, \mathbf{y}))$. \square

C Algorithmic variability of knockoffs

Despite the good average power of knockoffs, we find that it suffers generally poor stability with respect to knockoff resampling. Given data \mathbf{X}, \mathbf{y} , consider two independent draws of the knockoff matrix $\widetilde{\mathbf{X}}^{(1)}$ and $\widetilde{\mathbf{X}}^{(2)}$. These lead to two rejection sets $\mathcal{R}^{(r)} \equiv \mathcal{R}([\mathbf{X}, \widetilde{\mathbf{X}}^{(r)}], \mathbf{y})$, $r = 1, 2$. Their similarity can be measured via the *Jaccard Index*, defined

$$J(\mathcal{R}^{(1)}, \mathcal{R}^{(2)}) \equiv \frac{|\mathcal{R}^{(1)} \cap \mathcal{R}^{(2)}|}{|\mathcal{R}^{(1)} \cup \mathcal{R}^{(2)}|}.$$

This quantity is between 0 and 1, with higher Jaccard Indices representing greater similarity. We define the *stability* of the knockoffs rejection set $\mathcal{R}([\mathbf{X}, \widetilde{\mathbf{X}}], \mathbf{y})$ as the expectation of this quantity:

$$\text{stability}(\mathbf{X}, \mathbf{y}) \equiv \mathbb{E} \left[J \left(\mathcal{R}([\mathbf{X}, \widetilde{\mathbf{X}}^{(1)}], \mathbf{y}), \mathcal{R}([\mathbf{X}, \widetilde{\mathbf{X}}^{(2)}], \mathbf{y}) \right) \middle| \mathbf{X}, \mathbf{y} \right]. \quad (9)$$

To assess this measure of stability, we applied knockoffs with $\alpha = 0.1$ in a simulation setting with a sparse linear model with $p = 500$ Gaussian covariates and $n = 1000$ samples. We use an autocorrelated design matrix $\Sigma_{j_1, j_2} = \rho^{|j_1 - j_2|}$, with $\rho \in \{0.2, 0.5, 0.8\}$. The s non-null entries of the coefficient vector β are equally spaced, all have magnitude ν , and random signs. We repeat the experiment 25 times each for six signal strengths, $\rho \in \{0.2, 0.5, 0.8\}$, and $s \in \{25, 50, 100\}$. We

reran knockoffs for each experiment with 50 independently drawn knockoffs realizations. Then, we approximated the stability via

$$\widehat{\text{stability}}(\mathbf{X}, \mathbf{y}) \equiv \frac{1}{\binom{50}{2}} \sum_{1 \leq r_1 < r_2 \leq 50} J\left(\mathcal{R}([\mathbf{X}, \widetilde{\mathbf{X}}^{(r_1)}], \mathbf{y}), \mathcal{R}([\mathbf{X}, \widetilde{\mathbf{X}}^{(r_2)}], \mathbf{y})\right).$$

Figure A1 shows the stability of knockoffs rejections across different values of ρ and s . If only the null rejections changed with knockoff resampling, we would expect the stability to be $(1 - \alpha)/(1 + \alpha) \approx 0.82$, which is denoted by the dashed line in the figure. Aside from the extreme scenarios when the power is either very low or very high, the stability of the knockoffs rejection set generally fails to meet this threshold. This suggests that even the non-nulls rejected by knockoffs change based on the randomization.

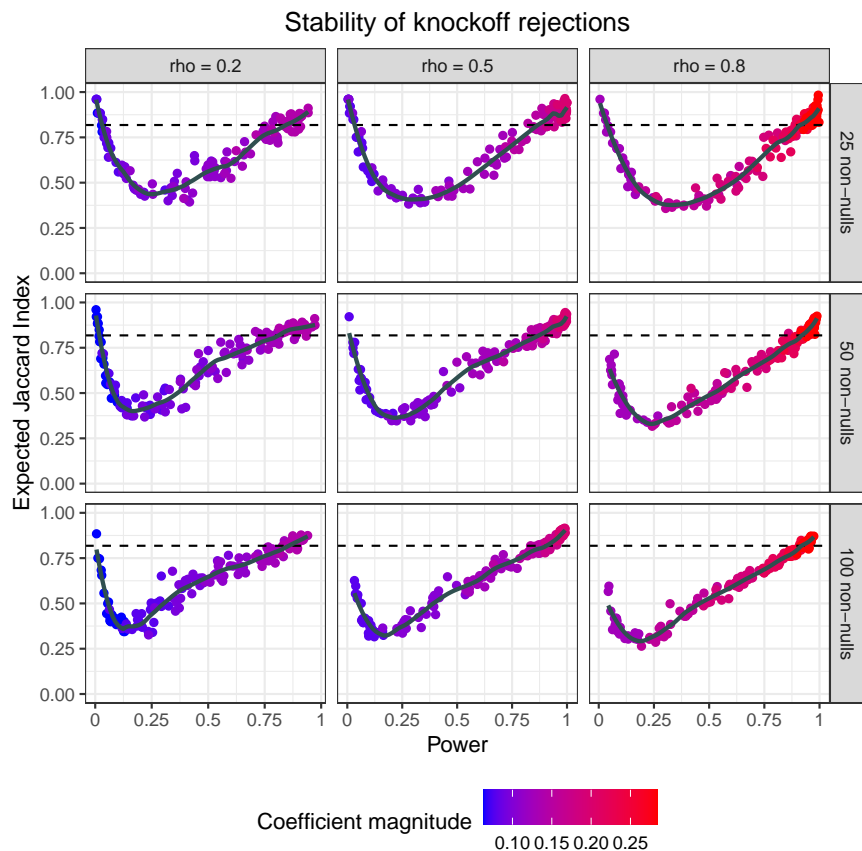


Figure A1: Expected similarity—measured using the Jaccard Index—between knockoff rejection sets resulting from two independent knockoff samples (see definition (9)). Each point corresponds to a realized pair (\mathbf{X}, \mathbf{y}) , generated from a sparse linear model with 1000 samples, 500 variables, s non-nulls, AR(1) Gaussian design with parameter ρ . There are 25 points (repetitions) each for six signal strengths, and the FDR level is $\alpha = 0.1$. LOESS smoother (gray) is added for visualization. Ideally, the Jaccard index would be around $(1 - \alpha)/(1 + \alpha) \approx 0.82$ (dashed line) if repeated runs lead to only the selected nulls changing with the selected non-nulls staying the same. The dip in the middle of each plot suggests high algorithmic variability in practical settings where the power is not very low or very high. This significant variability across re-runs is acknowledged to be a drawback of knockoffs from a reproducibility standpoint.

D Simulation results

In this section, we present the details of the simulations summarized in Section 4. Source code for conducting dCRT and other benchmark methods in our simulation studies can be found at <https://github.com/moleibobliu/Distillation-CRT>.

D.1 Method implementation details

We describe here the implementation choices and tuning parameters used for the main methods employed in our simulations; these descriptions apply everywhere to the simulated methods unless specifically stated otherwise. For many of our methods we use the lasso, which is implemented in the R package `glmnet` with `family="binomial"` if Y is binary and `family="gaussian"` otherwise, and penalty parameter selected by 10-fold cross-validation.

The d_0 CRT and d_1 CRT are the resampling-free versions of Examples 1 and 2, respectively. Note that the resampling-free dCRT may not be the most powerful choice for binary responses; we could have used a resampling-based univariate logistic regression statistic instead, but choose not to for computational purposes.

The dimension k in Examples 2 is set as $k = 2 \log(p)$. When we combine the dCRT methods with screening from Section 3.1, the screening is done by running the 10-fold-cross-validated lasso and keeping only the covariates with nonzero fitted coefficients.

The other methods we include are HRT and knockoffs (the last only in simulations targeting FDR control). We implement the HRT of Algorithm 1 in Tansey et al. (2018) with linear model fitted by the lasso, empirical risk function set to logistic loss for binary Y and sum of squared error otherwise, and a data split of 50%-50%. Due to data-splitting, the fitted lasso of the HRT is independent of the data used for hypothesis testing. Thus, the BH and Bonferroni correction procedures can be used on the p -values of the variables selected by the lasso, instead of on the full set of variables. This reduction of the multiplicity burden improves the power of the HRT, and we apply this screening step in all simulations and data analysis. In multiple testing simulations, BH is applied to the p -values of all methods except knockoffs. As we set $p \leq 800$ and FDR level $\alpha = 0.1$ for multiple testing, we set of the number of resamples $M = 50,000$ for the CRT approaches (CRT, HRT, non-resampling-free dCRTs). This choice was made to ensure these methods' powers are not affected by M , since $M/5 = 10,000 > p/\alpha$, the smallest possible BH cutoff in our simulations. The only exception is in Appendix D.3 where p reached as high as 3,200, and there we choose $M = 200,000$ to ensure $M/5 > p/\alpha$. For single hypothesis testing simulations where the significance level was 0.05, we set $M = 2,000$ to ensure that we still have $M > 1/0.05$. For knockoffs, we use the lasso coefficient difference statistics as defined in the (3.6) of Candès et al. (2018), the "knockoffs+" threshold, and the SDP knockoff construction when $p < 1000$ and the equicorrelated construction otherwise. We note that for both autocorrelated and equicorrelated variables, SDP and equicorrelated knockoffs are quite similar.

D.2 Moderate size data simulation

We first compare the dCRT with the original CRT procedure in Candès et al. (2018). We generate Gaussian covariates as auto-regressive of order 1 (AR(1)), with autocorrelation coefficient 0.5. The true model for Y is chosen as either a Gaussian linear model with unit residual variance or a logistic regression model, and in either case the coefficient vector was set to have s nonzero entries of equal magnitude ν and random signs (each independently having equal probability of being positive or negative). Two types of structures of the coefficient support are considered separately: adjacent

support with the first s coefficients being non-zero, and equally-spaced support with the non-zero coefficients indexed by $\{1, [p/s] + 1, 2[p/s] + 1, \dots, (s - 1)[p/s] + 1\}$. We pursue two multiple testing goals of selecting non-null variables while controlling the FDR or FWER, both at level $\alpha = 0.1$.

In addition to the methods described in Appendix D.1, we implement the original CRT with three different test statistics: the fitted coefficients of a linear or logistic lasso regression, elastic net (Zou and Hastie, 2005) regression (penalty $\lambda(\|\beta\|_1 + \|\beta\|_2^2/2)$), and adaptive lasso regression (Zou, 2006; Huang et al., 2008), each tuned with 10-fold cross-validation. Due to the high computational burden of these CRTs, we focus on moderate size data with $n = 300$, $p = 300$ and the sparsity level $s = 30$ and vary ν to observe a range of powers.

The resulting average power in the linear and logistic settings is plotted against the signal magnitude ν in Figure A2 for FDR control and Figure A3 for FWER control, and the FDR plots are presented in Appendix D.11. All methods control the FDR. For both FDR and FWER control, the d_0 CRT and d_1 CRT significantly outperform the HRT for both types of support, perform better than knockoffs and all the CRT methods for adjacent support but worse than them for equally spaced support. The d_1 CRT has slightly less power than the d_0 CRT due to its allowance of interaction effects, since the true model is exactly additive.

To study and compare the computational efficiency of the methods, we present in Table A1 the average computation time of the methods, with all algorithms implemented in R. Compared with the original CRT procedures, the dCRTs drastically reduce the computation time and are thus much more user-friendly. Knockoffs and the HRT use less time than dCRT because they only fit a high dimensional regression once.

Average computation times (minutes)							
	d_0 CRT	d_1 CRT	knockoff	HRT	CRT(lasso)	CRT(ElaNet)	CRT(Ada)
Linear	0.6	0.6	0.2	0.3	355.9	425.5	378.9
Logistic	1.7	1.8	0.1	0.5	309.0	461.0	391.8

Table A1: Average computation times (in minutes) of the $n = p = 300$ simulations of Appendix D.2. dCRT is much more efficient than the CRT, and slightly more expensive than knockoffs and HRT.

D.3 Large size data simulation

In this section, we conduct simulation studies of a scale beyond the CRT’s computational feasibility, and hence focus on the remaining methods whose computation stays manageable. As a baseline, we set $n = p = 800$, again use AR(1) covariates with autocorrelation 0.5, generate Y from Gaussian linear model with unit residual variance, and use a coefficient vector with $s = 50$ nonzero entries of equal magnitude $\nu = 0.175$ (chosen to make the power around 0.5) and random signs (each independently having equal probability of being positive or negative). Again, the adjacent and equally-spaced supports are studied separately and we pursue controlled variable selection with nominal FDR or FWER $\alpha = 0.1$.

Each of the four average power plots in Figure A4 varies one the parameters (ν , n , p , or s) from this baseline simulation setup, with the ranges given by the x-axes. The two dCRTs have similar performance, both of them outperform the HRT in all cases for both FDR and FWER control. They perform better than knockoffs for adjacent support but worse than knockoffs for equally-spaced support under most cases. When the sparsity level s is below 10, the power of knockoffs drops to 0 because of the effect mentioned in Section 4.

We present the average computation times when $n = 800$, $p = 800$ and $s = 50$ in Table A2.

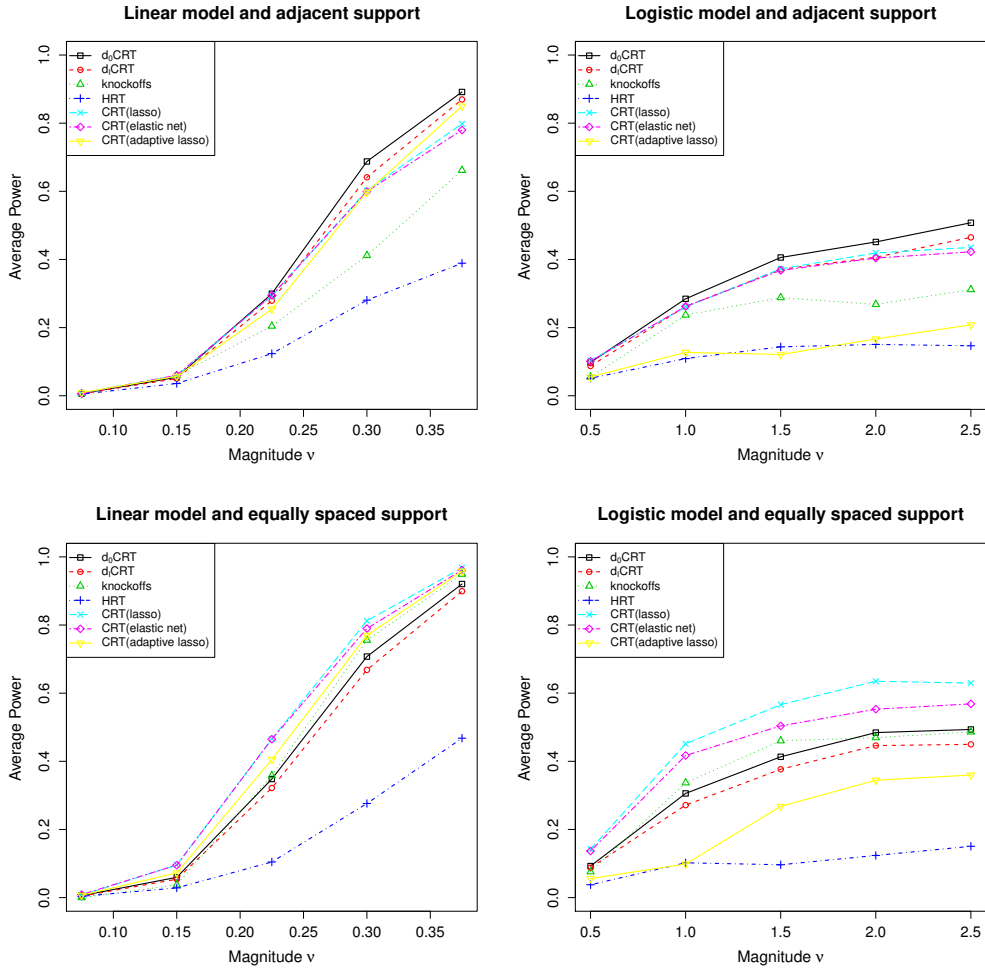


Figure A2: Average powers of FDR control of the $n = p = 300$ simulation of Appendix D.2. All standard errors are below 0.01 and are hence excluded. The d CRT approaches are the most powerful for adjacent support but slightly worse than CRT methods and knockoffs for equally spaced support.

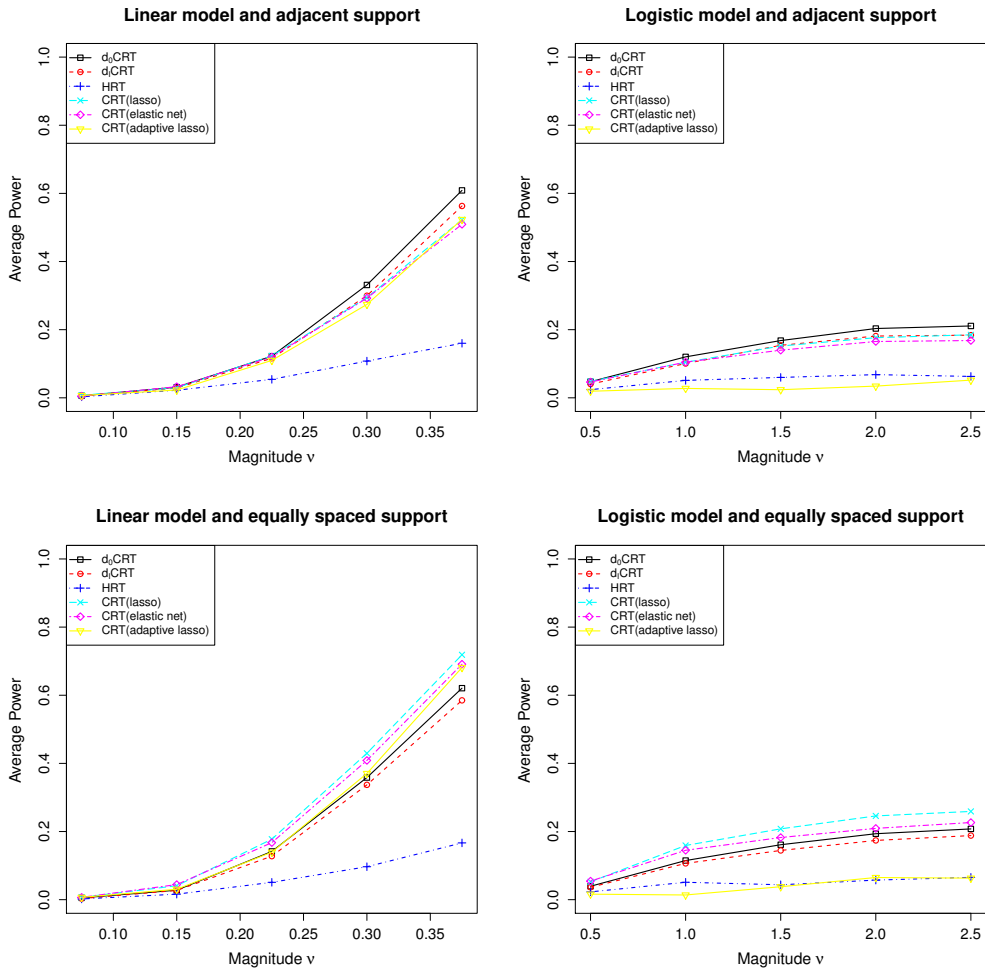


Figure A3: Average powers of FWER control of the $n = p = 300$ simulation of Appendix D.2. All standard errors are below 0.01 and are hence excluded. The d CRT approaches are the most powerful for adjacent support but slightly worse than CRT methods for equally-spaced support.

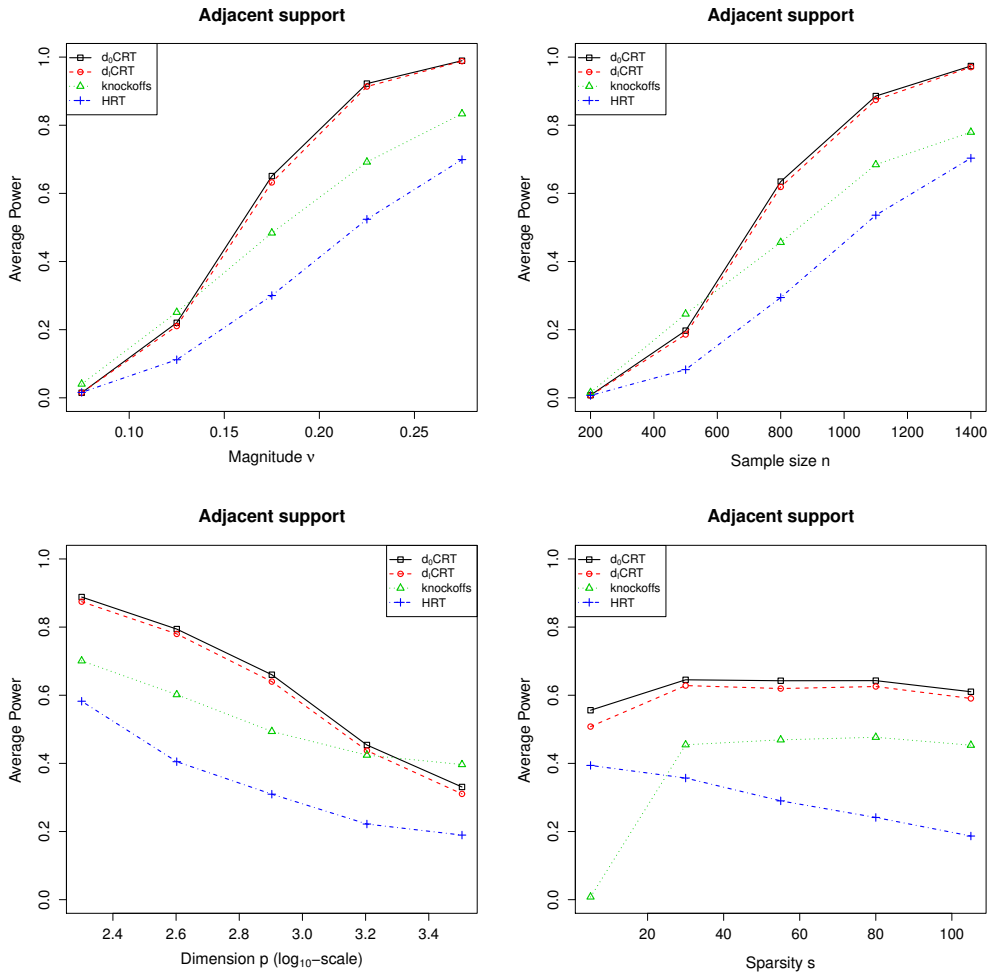


Figure A4: Average powers of FDR control of the large scale simulations of Appendix D.3 that vary the coefficient magnitude, sample size, dimension, and coefficient sparsity with adjacent support. All standard errors are below 0.01. Our dCRT approaches are typically the most powerful.

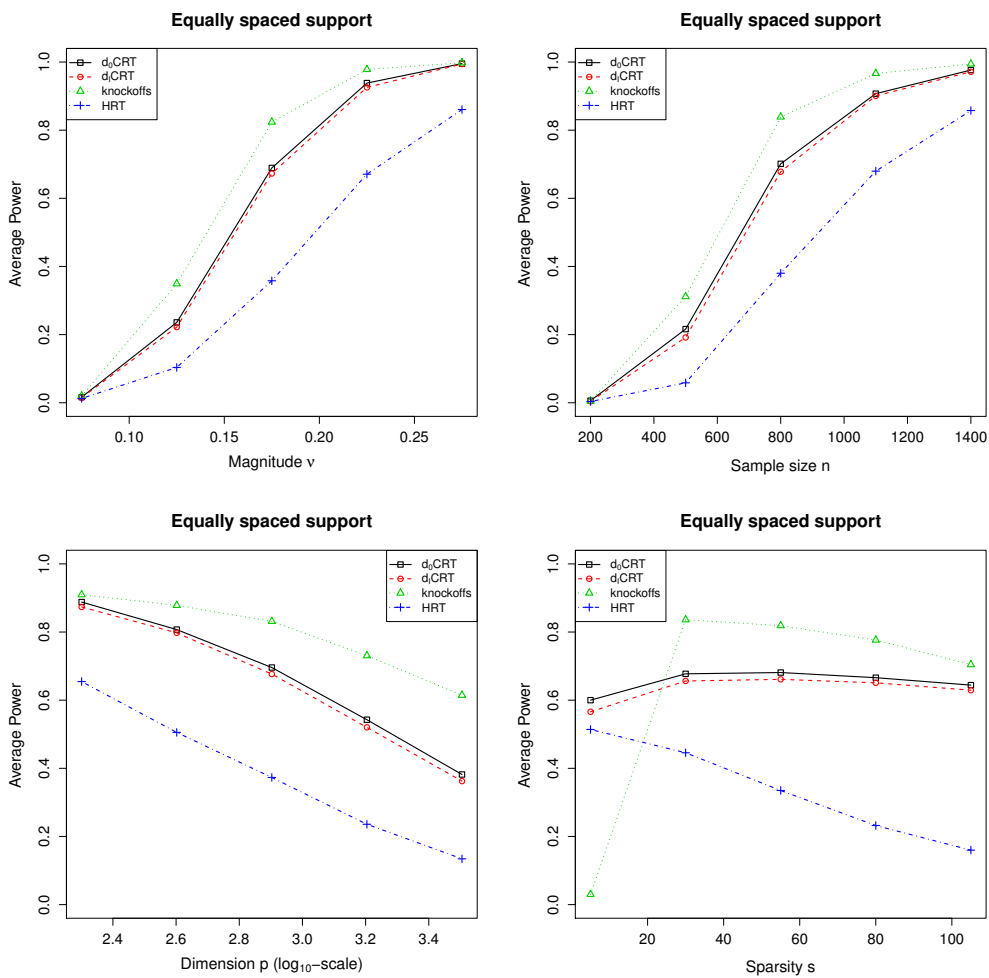


Figure A5: Average powers of FDR control of the large scale simulations of Appendix D.3 that vary the coefficient magnitude, sample size, dimension, and coefficient sparsity with equally spaced support. All standard errors are below 0.01. The dCRTs have lower power than knockoffs in most cases.

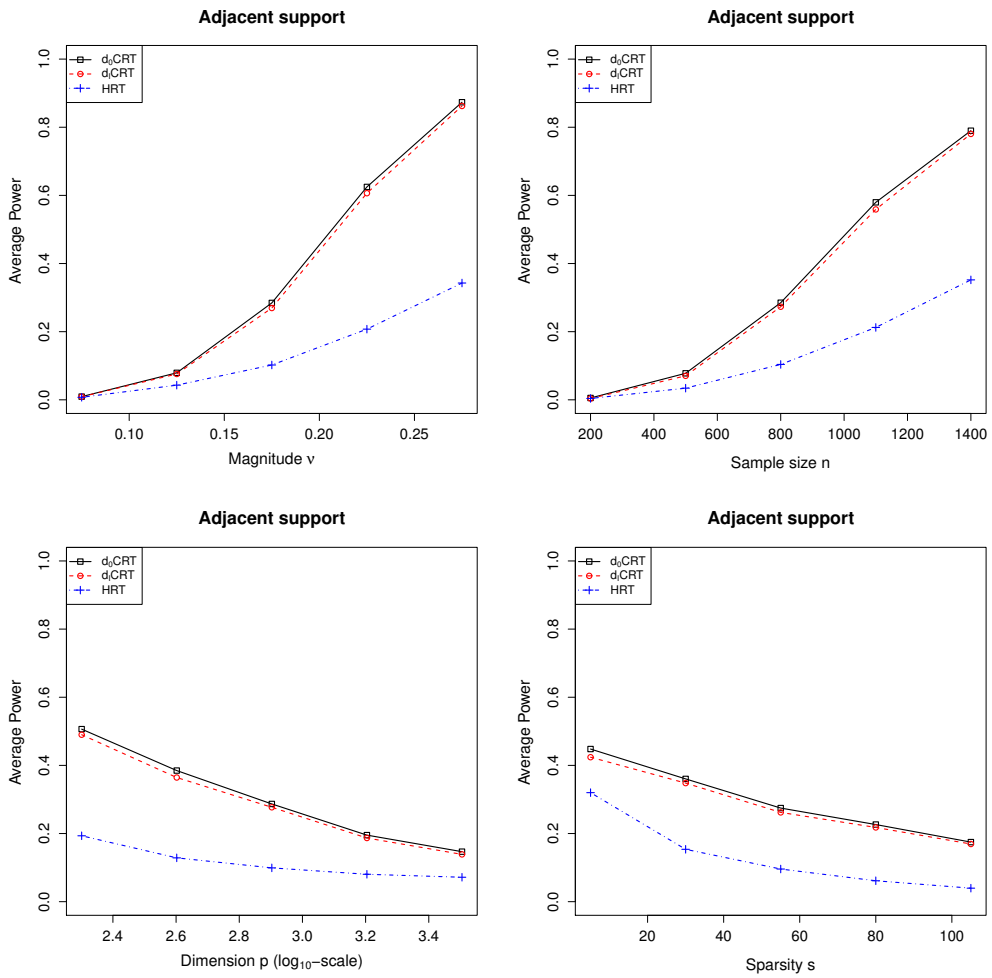


Figure A6: Average powers of FWER control of the large scale simulations of Appendix D.3 that vary the coefficient magnitude, sample size, dimension, and coefficient sparsity with adjacent support. All standard errors are below 0.01. The dCRTs are more powerful than the HRT.

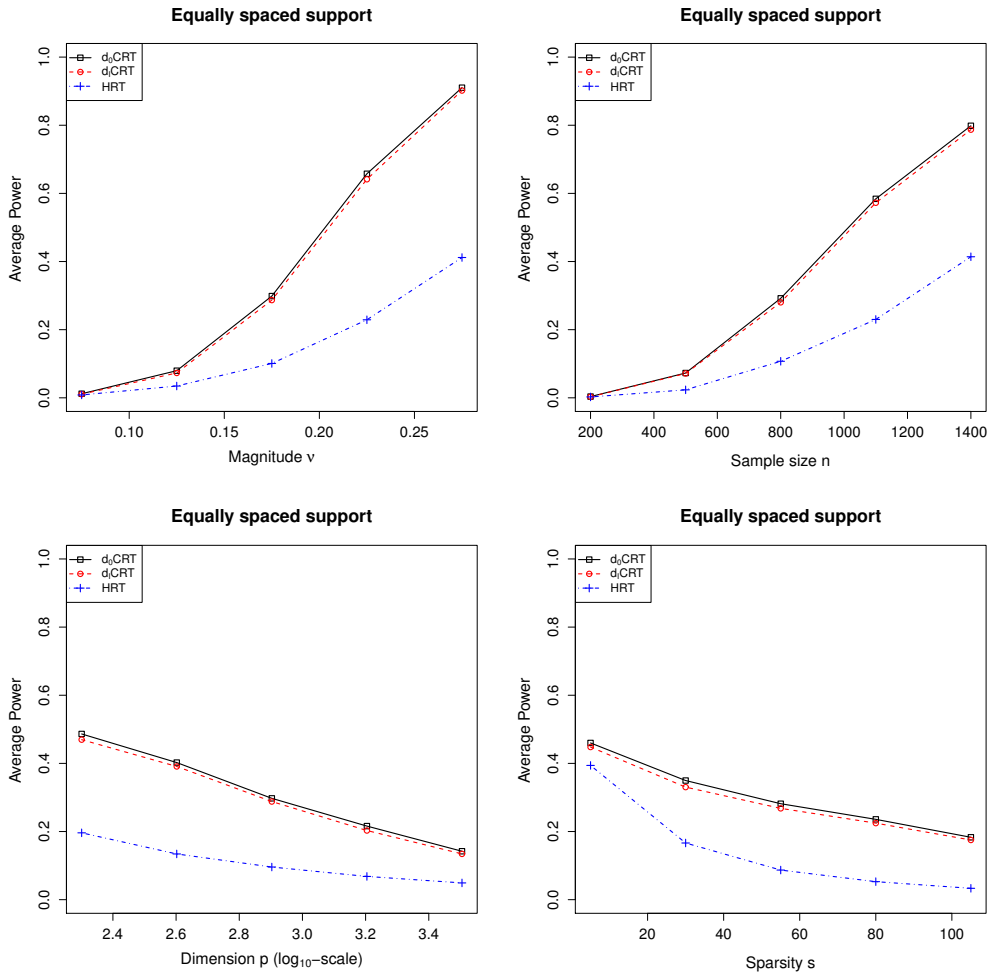


Figure A7: Average powers of FWER control of the large scale simulations of Appendix D.3 that vary the coefficient magnitude, sample size, dimension, and coefficient sparsity with equally spaced support. All standard errors are below 0.01. The dCRTs are more powerful than the HRT.

Knockoffs and HRT still run faster than the dCRT methods since they only fit high dimensional model once in the whole procedure.

Average computation times (minutes)			
d ₀ CRT	d ₁ CRT	knockoffs	HRT
9.8	10.2	1.8	6.2

Table A2: Average computation times (in minutes) of the $n = p = 800$ simulations of Appendix D.3. As expected, knockoffs is the fastest, while dCRT is slightly slower than the HRT.

We now study varying the covariate and response models from this same baseline simulation. First we generate Gaussian covariates with covariance structure set as AR(1) with autocorrelations 0.25, 0.5, and 0.75, and equicorrelated with correlations 0.15, 0.3, and 0.45. Second we generate Y from three additional models given by:

- (i) **Poisson model:** Y is generated from a Poisson GLM with the same coefficient vector as the baseline model.
- (ii) **Logistic model:** Y is generated from a logistic regression with the same coefficient vector as the baseline model except $\nu = 0.5$.
- (iii) **Polynomial model:** Y is generated from a Gaussian model with conditional mean given by a polynomial that starts from the baseline model with $\nu = 0.105$ and takes each covariate with a nonzero coefficient and adds a term equal to 0.3 times its cube.

The signal magnitudes of each setting are chosen to make the powers of the main methods close to 0.5, for convenience of comparison. Note that under (i) and (iii), we still fit linear lasso, though the model is wrong. The resulting average powers of both these simulations are plotted in Figure A8. The d₀CRT and d₁CRT have significantly higher power than HRT in all settings. The comparison to knockoffs is more complicated. Knockoffs generally performs worse under adjacent support and under spaced support with equicorrelated design, suggesting that knockoffs is sensitive to correlations among signal variables. On the other hand, dCRT performs worse under highly autocorrelated designs. These subtle differences are intriguing and we leave their further investigation to future work. Again, all the methods control FDR properly with the desired level 0.1 in the numerical studies corresponding to Figures A4 and A8, and we present the FDR plot in Appendix D.11.

D.4 Comparing dCRT with DML and GCM

As mentioned in the introduction, the test statistic of the resampling-free d₀CRT is quite similar to that of DML (Chernozhukov et al., 2016) and GCM (Shah and Peters, 2018) when X is Gaussian. However, we remind the reader that both DML and GCM rely on asymptotic normality to calibrate their tests, requiring large samples and well-behaved tails for validity. By comparison, CRT-based methods including the dCRT and HRT are valid in finite samples for any data distribution.

We demonstrate this difference by setting $n = 30$, $p = 100$ and drawing each covariate independently from a Laplace distribution with mean 0 and variance 2/9. We generate Y from a linear model with the residual ϵ also drawn from the Laplace distribution of mean 0 and variance 1/2. Our target is again multiple testing with FDR level 0.1. We compare HRT, DML, GCM and dCRT. When implementing DML and GCM, we use our assumed exact model- X knowledge to construct the exact partial residual for each covariate, and use the lasso on (\mathbf{y}, \mathbf{Z}) to obtain the partial residuals for Y . For DML, we use 8-fold cross-fitting. The resulting FDRs are presented

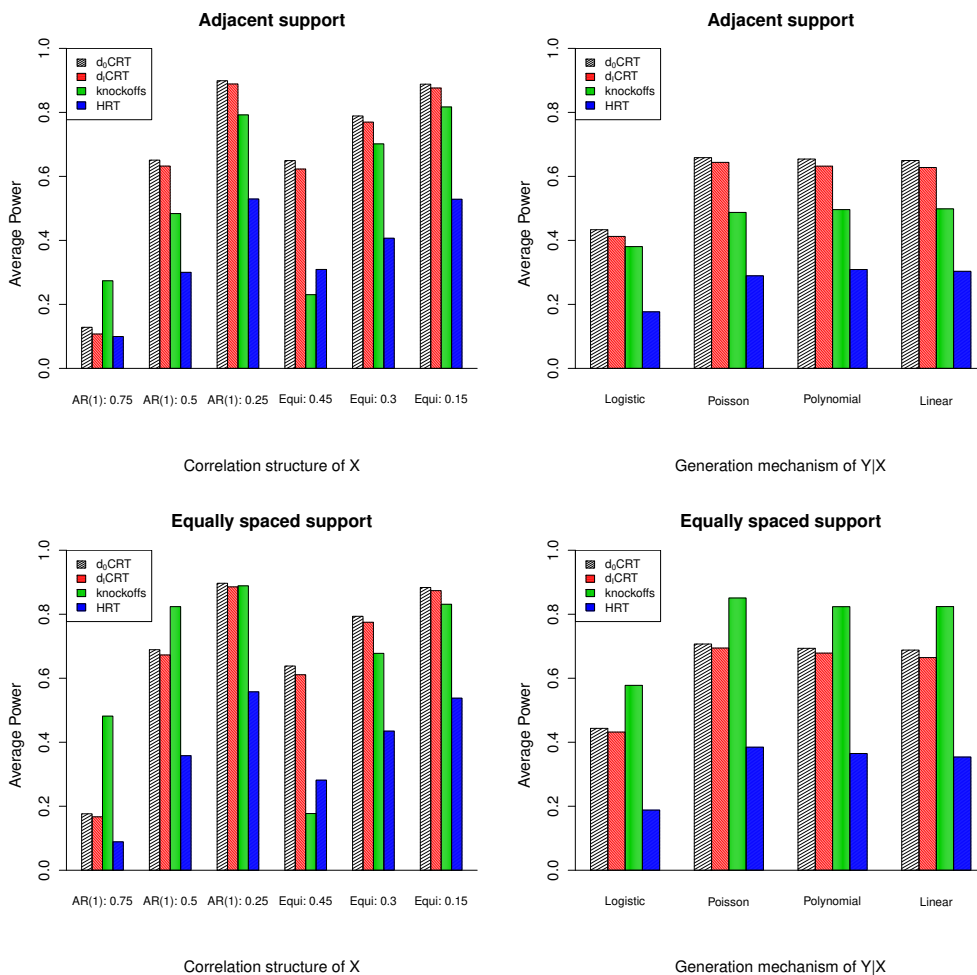


Figure A8: Average powers of the large scale simulations of Appendix D.3 that vary the covariate and response models; all standard errors are below 0.01. The d CRTs have higher power than knockoffs in most scenarios with adjacent support or equicorrelated design, lower power than knockoffs for equally-spaced support and autocorrelated design, and consistently higher power than HRT.

in Figure A9. Both DML and GCM have FDR level substantially above the nominal 0.1 under all magnitudes, while HRT and dCRT still control the FDR below 0.1 (as guaranteed by Theorem 1).

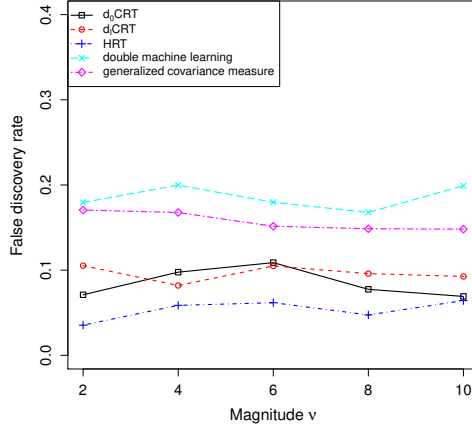


Figure A9: False discovery rates of the simulation in Appendix D.4 comparing computationally efficient CRT methods to DML and GCM. All standard errors are below 0.01. DML and GCM do not control the FDR at the target level 0.1, but the other methods do.

D.5 Power improvement of the d₁CRT in the presence of interactions

All previous simulations have shown similar, if slightly worse, performance for the d₁CRT compared to the d₀CRT. This is because the models have all been additive (technically a logistic regression model is not additive, but the logistic-regression-derived statistics used by both dCRT methods fit to the logistic-transformed Y , which does follow an additive model). To demonstrate the benefits of the d₁CRT to characterize more complex effects, we conduct here a non-additive simulation with first-order interactions that obey the hierarchy principle described in Section 2.3.2. We take $n = p = 800$ and generate $(X, Z^T)^T$ from AR(1) with autocorrelation 0.5. Letting $\mu(X, Z) = \nu(X + \sum_{k=1}^5 Z_{j_k} + 1.5X \sum_{k=1}^5 Z_{j_k})$ with j_1, \dots, j_5 randomly picked from $\{1, 2, \dots, 799\}$, we generate Y either from a Gaussian model with conditional mean given by $\mu(X, Z)$ or from a Bernoulli model with $\log(\mathbb{P}(Y = 1 | X, Z) / \mathbb{P}(Y = 0 | X, Z)) = \mu(X, Z)$. The target is to test the single hypothesis $Y \perp X | Z$ at level 0.05 (hence knockoffs does not apply). Figure A10 shows the powers of the d₀CRT, d₁CRT, and HRT. As is expected, d₁CRT has substantially higher power than d₀CRT.

D.6 Stability of the d₁CRT to the choice of k

In this section, we study the sensitivity of d₁CRT to the choice of k defined in Example 2. We simulate the d₁CRT in the baseline setting (linear model) of Section D.3 and the linear interaction model setting of Section D.5 for varying choices of k (in both settings, the default $k = 2 \log(p) \approx 13$). The results in Figure A11 show that the choice of k has nearly no impact on the power of the d₁CRT in the linear model setting. In the interaction setting, the power of the d₁CRT decreases with k for $k > 5$ since there are only 5 true interactions in the model, but the trend is quite gradual and the d₁CRT's power stays above that of d₀CRT through $k = 22$.

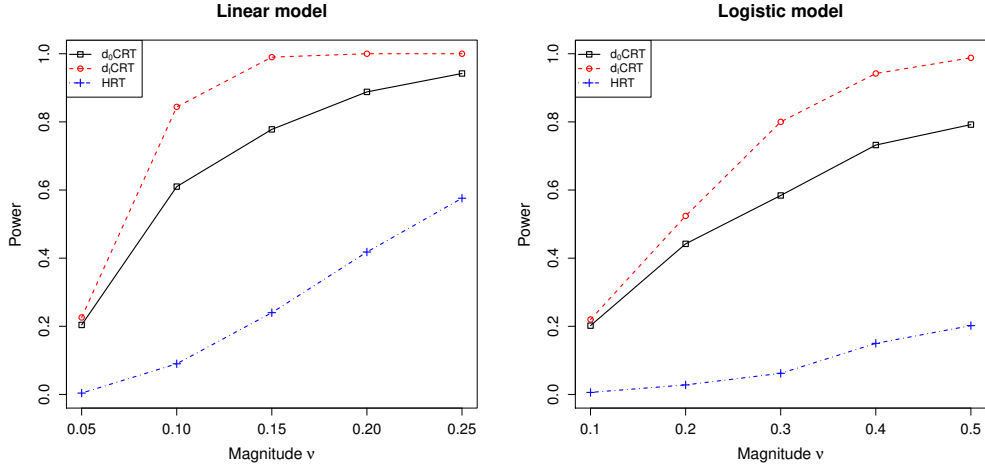


Figure A10: Powers of the simulations in Appendix D.5 comparing methods in the presence of interactions; standard errors are below 0.03. The d_1 CRT is much more powerful than the HRT.

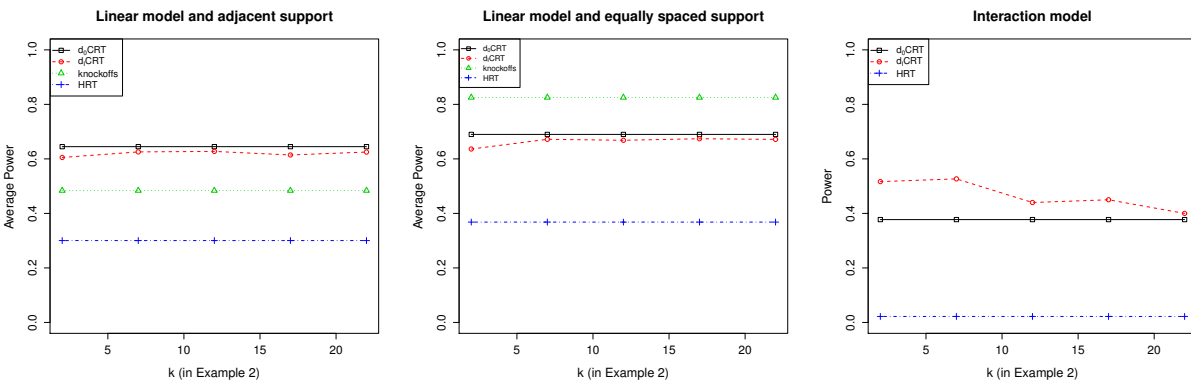


Figure A11: Powers of the simulation in Appendix D.6 evaluating the stability of the d_1 CRT to the choice of k ; all standard errors are below 0.03. The d_1 CRT is fairly stable to the choice of k .

D.7 A random-forest-based d_1 CRT

Examples 1 and 2 are inherently rooted in generalized linear models (GLMs), and we expect them to perform well in situations where a GLM captures much of the interesting dependence between Y and X . But there is nothing limiting the d CRT’s application to such settings, and in this section we demonstrate the power of a random-forest-based d_1 CRT in a setting that is far from a GLM.

Example 3 (Random-forest-based d_1 CRT). Let $\mathbf{d}_{y,1}$ be the fitted predictions from a random forest fitting \mathbf{y} to \mathbf{Z} , let $\mathbf{d}_{y,-1}$ be the columns of \mathbf{Z} corresponding to the k largest values of the default variable importance measure in the R package `randomForest`, and let $T(\mathbf{y}, \mathbf{x}, \mathbf{d}_y, \mathbf{d}_x)$ fit a random forest of \mathbf{y} on $\mathbf{x} - \mathbf{d}_x$ and \mathbf{d}_y and return the default variable importance measure for $\mathbf{x} - \mathbf{d}_x$.

We take $n = p = 800$ and $(X, Z^\top)^\top$ as following an AR(1) model with autocorrelation 0.5. We choose a conditional model for Y in which the magnitude of the effect of X on Y is heterogeneous and varies with Z : $\mu(X, Z) = \nu[0.5X^2 + \sin(0.5\pi X)](0.3 + \sum_{k=1}^5 Z_{j_k})$, and Y is standard normal noise added to $\mu(X, Z)$. We simulate tests of $Y \perp\!\!\!\perp X \mid Z$ at significance 0.05 and plot the results in Figure A12. The random-forest-based d_1 CRT is denoted by “ d_1 CRT (RF)” and uses 100 trees for distillation and 30 trees for computation of T . The additional function-approximation flexibility of random forests imparts a substantial gain in power compared to d_0 CRT, d_1 CRT, HRT, which are all implemented based on GLMs.

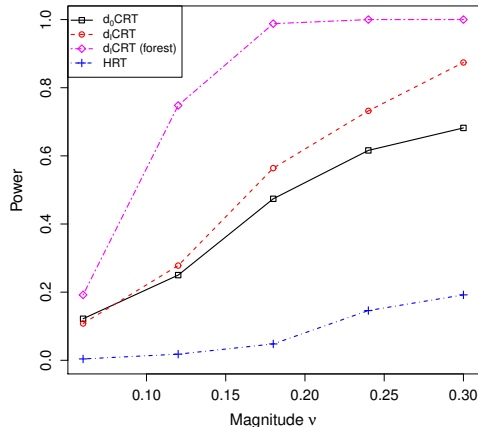


Figure A12: Powers of the simulations in Appendix D.7 demonstrating a random-forest-based d_1 CRT on a complex ground truth model; all standard errors are below 0.03. The flexibility of the random forest variant makes it much more powerful than the GLM-based d_0 CRT and d_1 CRT.

D.8 Robustness

We designed numerical experiments to study the robustness of the d CRTs, i.e., whether the methods still control Type-I error and have power when the $X \mid Z$ distribution is misspecified.

D.8.1 Known first and second moments

We first consider the case when one has no knowledge of the conditional distribution of $X \mid Z$ except its first two moments, and simply treats $X \mid Z$ as conditionally Gaussian with matching

moments. We let $n = p = 800$ and generate $Z = (Z_1, Z_2, \dots, Z_{799})^\top$ from a Gaussian AR(1) model with autocorrelation 0.5 and sample X as conditionally Poisson:

$$X = 0.15 \sum_{j=1}^{50} \varphi_j Z_j + \delta, \quad \text{where } \delta = \frac{O - r}{\sqrt{r}} \quad \text{with } O | Z \sim \text{Poi}(r),$$

where each φ_j is independently and uniformly drawn from $\{-1, 1\}$ and $\text{Poi}(r)$ represents the Poisson distribution with mean r . When r is small, $(O - r)/\sqrt{r}$ is quite skewed with its tail behaviour highly different from Gaussian while as r becomes larger, $(O - r)/\sqrt{r}$ converges to a $\mathcal{N}(0, 1)$. We run the dCRT as if $\delta \sim \mathcal{N}(0, 1)$, and hence r measures the degree of misspecification (lower r corresponds to more misspecification). For Y , we use linear or logistic model linked with $\nu X + 0.15 \sum_{j=1}^{50} \psi_j Z_j$.

Our target is to test for $Y \perp\!\!\!\perp X | Z$ with level 0.05. To study the performance in Type-I error control we set $\nu = 0$, while to study the power we let $\nu = 0.1$ for linear model and $\nu = 0.2$ for logistic model. We compare $d_0\text{CRT}$, $d_1\text{CRT}$, and HRT, with the same specification as the previous section except that $X - \mathbb{E}[X|Z]$ is approximated as $\mathcal{N}(0, 1)$ when modelling X . The resulting Type-I error and power versus $\log_2(r)$ are plotted in Figure A13. Even when r is as small as 0.5, the Type-I error of the dCRTs remain below their nominal level and their powers are relatively similar to the nearly-well-specified setting of $r = 64$.

D.8.2 In-sample-estimated moments

Next, we study the case when one knows a model family for $X | Z$ but needs to estimate its parameters in-sample. Again, we set $n = 800$, $p = 800$, $s = 50$, generate the covariates from a Gaussian AR(1) distribution with autocorrelation 0.5 and generate Y from a linear model with magnitude $\nu = 0.175$ or logistic model with magnitude $\nu = 0.5$, which again makes the power roughly 0.5. Then, as part of our dCRT procedures, we use the $n = 800$ samples to estimate the precision matrix of the covariates. For this purpose, we implement the graphical lasso (Friedman et al., 2008, glasso) tuned by cross-validation. Given the true sparsity of this particular covariate model, the glasso does relatively well, so we also try mixing its covariance matrix estimate $\hat{\Sigma}_g$ with the sample covariance matrix $\hat{\Sigma}$, which is a very poor estimate since $n = p$.

$$\hat{\Sigma}_m = D\{v\hat{\Sigma} + (1 - v)\hat{\Sigma}_g\}D,$$

where $v \in [0, 1)$ is a proportion parameter controlling the mixture of the two estimates and $D = \text{diag}\{d_1, d_2, \dots, d_p\}$ is a $p \times p$ diagonal matrix, where d_j is the ratio of the estimated conditional variance by inverting $v\hat{\Sigma} + (1 - v)\hat{\Sigma}_g$ and that estimated using the mean squared residuals. Here D is just used to ensure that the estimated conditional variance is close to its sample mean squared residual. By changing v , we are able to inspect the performance of the dCRT as the quality of our covariance estimation varies.

The goal of the simulation is is controlled variable selection with FDR level 0.1. The resulting FDR and power versus v are presented in Figure A14 for adjacent support and in Figure A15 for equally-spaced support. As the estimation error gets worse, knockoffs becomes conservative and its FDR and power drop. However, the dCRTs become slightly anticonservative as the estimation gets worse, achieving a somewhat inflated FDR but maintaining closer power to the setting with better estimation at $v = 0$, where they appear to behave exactly as if the covariance matrix were known exactly.

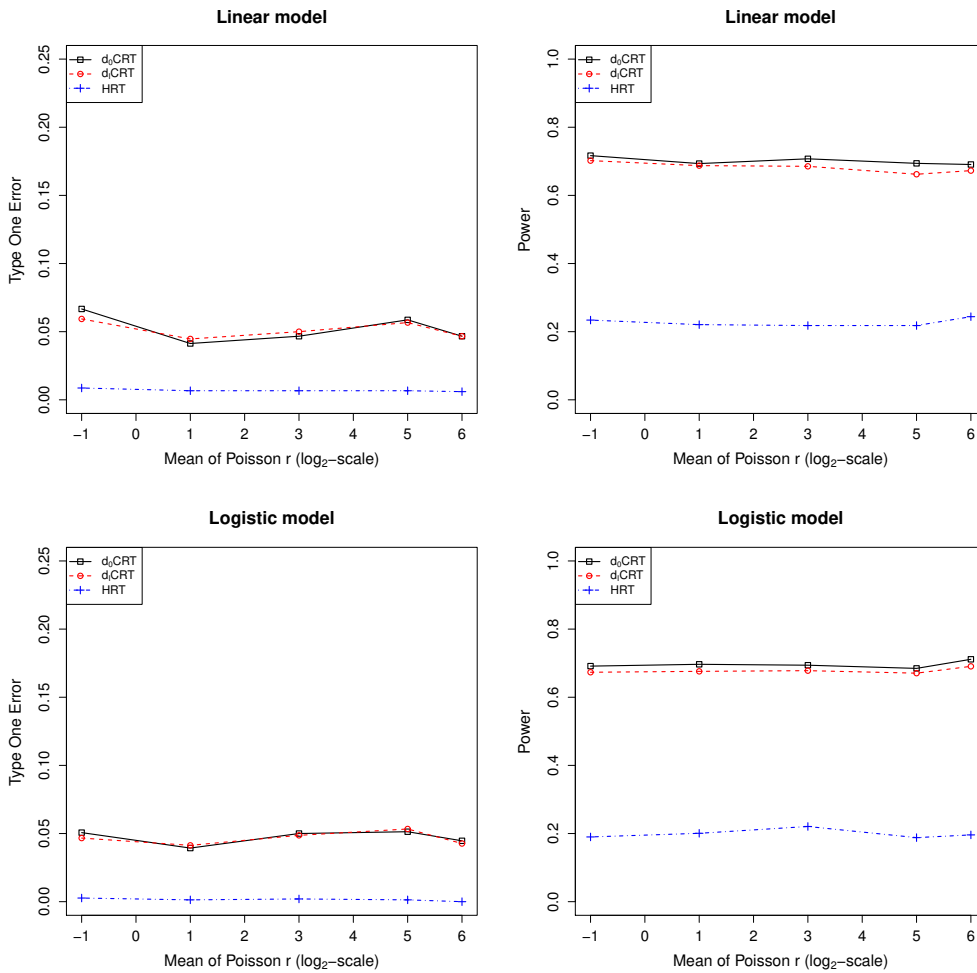


Figure A13: Type-I error rates and powers of the simulations in Appendix D.8.1 measuring robustness to misspecification in terms of the parameter r . All standard errors are below 0.03. All methods control Type-I error, and the dCRTs are more powerful than HRT.

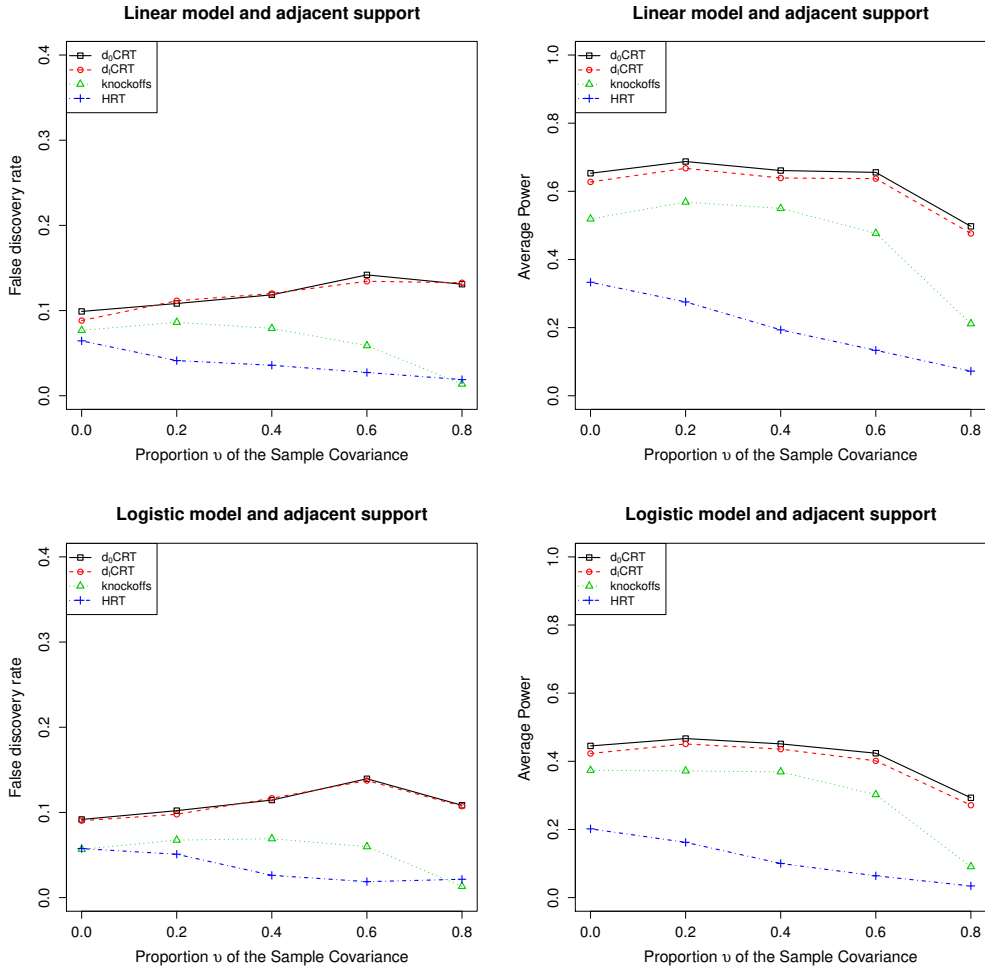


Figure A14: FDRs and average powers of the simulations in Appendix D.8.2 measuring robustness to in-sample estimation of the covariate covariance matrix. The true coefficients are generated with adjacent support. All standard errors are below 0.01. The FDR seems relatively unaffected by estimation of the covariance matrix, and the d CRTs are most powerful.

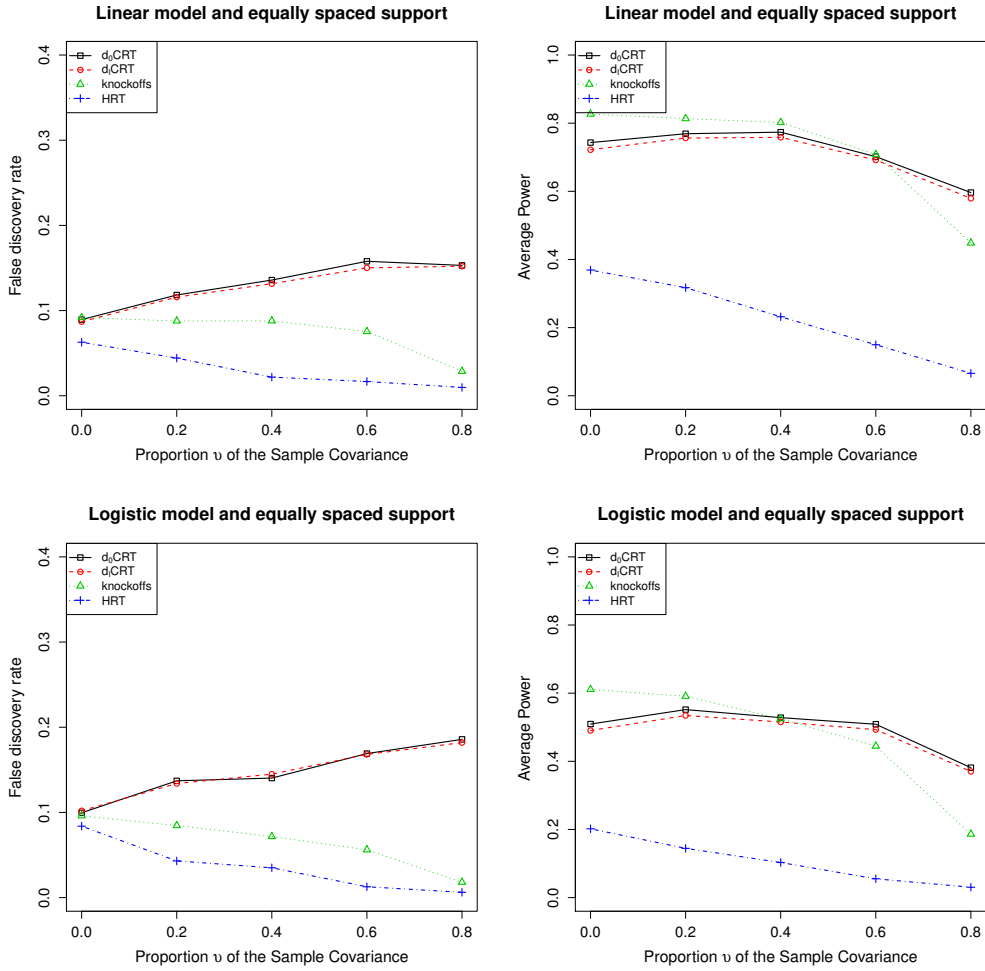


Figure A15: FDRs and average powers of the simulations in Appendix D.8.2 measuring robustness to in-sample estimation of the covariate covariance matrix. The true coefficients are generated with equally spaced support. All standard errors are below 0.01. The FDR seems relatively unaffected by estimation of the covariance matrix, and the d CRTs are most powerful in most cases.

D.9 Measuring the effect of the resampling-free modification

D.9.1 Gaussian covariates

Section 2.4 proposes a resampling-free version of d_0 CRT and d_1 CRT requiring a small modification to their test statistics; we show here this modification does not affect their powers. Under the baseline setting of Section D.3 and the setting with Gaussian covariates and interactions in Section D.5, we compare the resampling-free dCRTs with their non-resampling-free versions in terms of average power. Figure A16 shows the resampling-free modification makes essentially no difference to their powers.

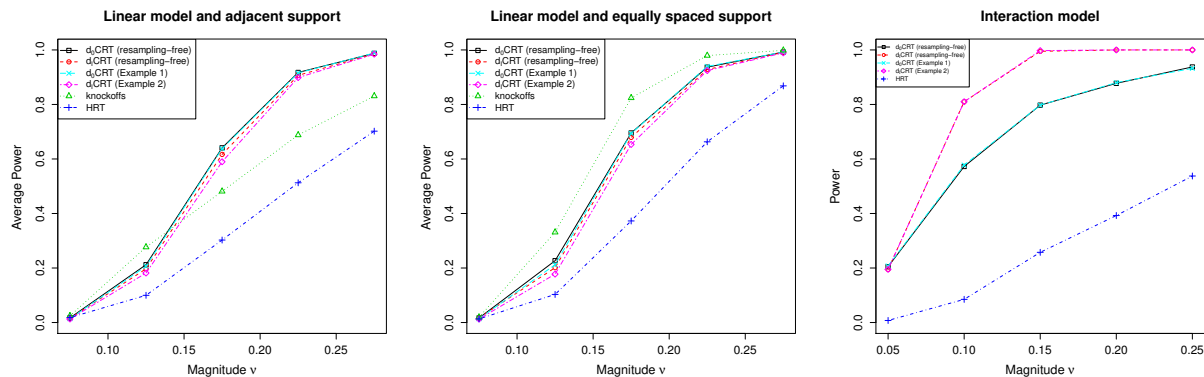


Figure A16: Powers of the simulation in Appendix D.9.1 measuring the effect of the resampling-free modification to the d_0 CRT and d_1 CRT test statistics; all standard errors are below 0.03. The resampling-free modifications of the dCRT have essentially the same power as the resampled versions.

We also include computation times for the baseline setting of Section D.3 in Table A3, showing that the resampling-free versions of the dCRTs confer a substantial computational savings.

Average computation times (minutes)					
d_0 CRT (resampling-free)	d_0 CRT (Example 1)	d_1 CRT (resampling-free)	d_1 CRT (Example 2)	knockoff	HRT
9.8	26.1	10.2	120.7	1.8	6.2

Table A3: Average computation times of the linear model simulations of Appendix D.9.1. The resampling-free modifications of the dCRT lead to considerable runtime savings.

D.9.2 Non-Gaussian covariates

As we introduced in Section 2.4 and detailed in Appendix A, when $X | Z$ is non-Gaussian, it must be transformed to Gaussian in order to apply the resampling-free speedup; we examine here the effect this transformation has on power. We generate covariates i.i.d. from two different distributions: (i) Gamma with shape 3 and rate 0.5 and (ii) Bernoulli with mean 0.5. We took $n = p = 800$, $s = 50$ and Y generated from linear (in the untransformed covariates) model and performed multiple testing for variable selection at FDR level 0.1. Our main goal is to compare the d_0 CRT of Example 1 and the d_1 CRT of Example 2 with their respective resampling-free counterparts, though we also run the HRT and knockoffs. The resulting average powers versus signal strength ν are shown in

Figure A17. For Gamma X , the Gaussian transformation comes with almost no loss in power while for Bernoulli X , the resampling-free dCRTs lose substantial power but still outperform the HRT. This is due to the highly non-Gaussian nature of a Bernoulli(0.5) distribution and the need for substantial exogenous randomness to be added to X to make it Gaussian. Knockoffs performs competitively with the dCRT methods in both simulations, and we attribute this to the covariate independence which allows very high-quality knockoffs to be used.

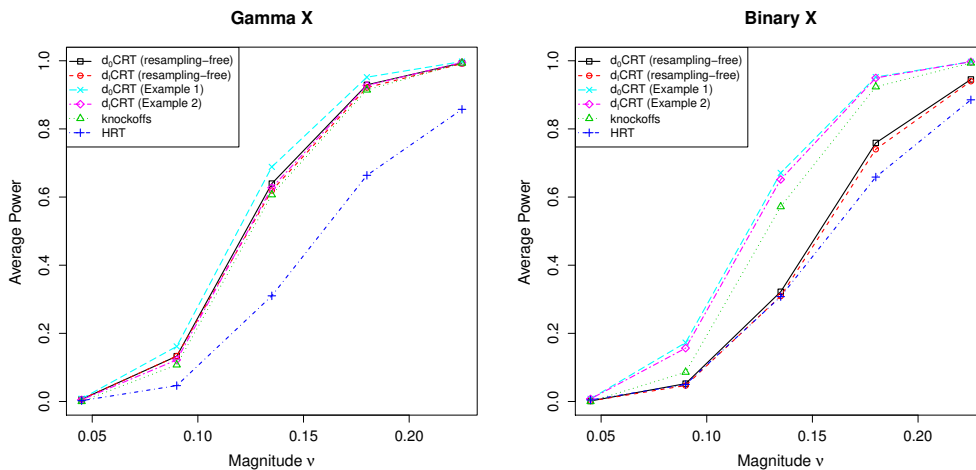


Figure A17: Powers of the simulation in Appendix D.9.2 measuring the effect of the Gaussian transformation in the resampling-free dCRTs. All standard errors are below 0.01. The dCRT resampling-based approaches have the most power in non-Gaussian settings as well, but the resampling-free modifications have lower power in the binary case.

D.10 Impact of screening on computation efficiency and power

Here we demonstrate the effect of the screening modification introduced in Section 3.1 on computation time and power. We again simulate the baseline setting in Section D.3 and compare the power and computation time of the dCRT methods with screening with the dCRT procedures without using screening. In Table A4 we present computation times demonstrating that screening can substantially improve the computational efficiency of dCRT. And the corresponding average powers are shown in Figure A18, demonstrating that screening has nearly no impact on the power of the d_0 CRT or d_1 CRT.

Average computation times (minutes)					
d_0 CRT (screening)	d_0 CRT (full)	d_1 CRT (screening)	d_1 CRT (full)	knockoff	HRT
9.8	46.1	10.2	47.1	1.8	6.2

Table A4: Average computation times (in minutes) of the simulations in Appendix D.10. Screening leads to large computational savings at nearly no cost to the statistical power.

D.11 Additional FDR results

We compile FDR results of our simulations with well-specified covariate distributions here. The FDR is guaranteed to be controlled by knockoffs and the p -values of the CRT procedures including

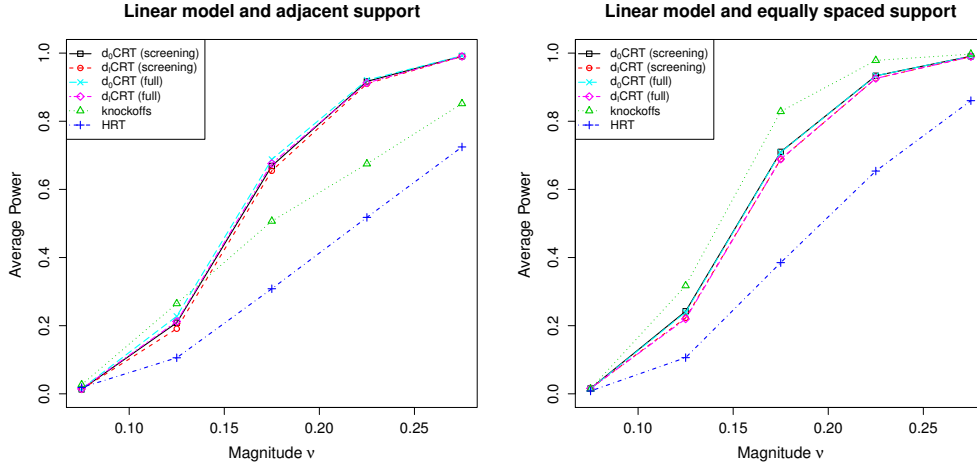


Figure A18: Average powers of the simulation in Appendix D.10 measuring the effect of the screening modification. All standard errors are below 0.01. The screened dCRTs have identical power to the dCRTs without screening, as expected.

the dCRTs are guaranteed to be valid, but they do not satisfy the conditions for the BH procedure to control the FDR. In practice, they do, as Figures A19–A22 show.

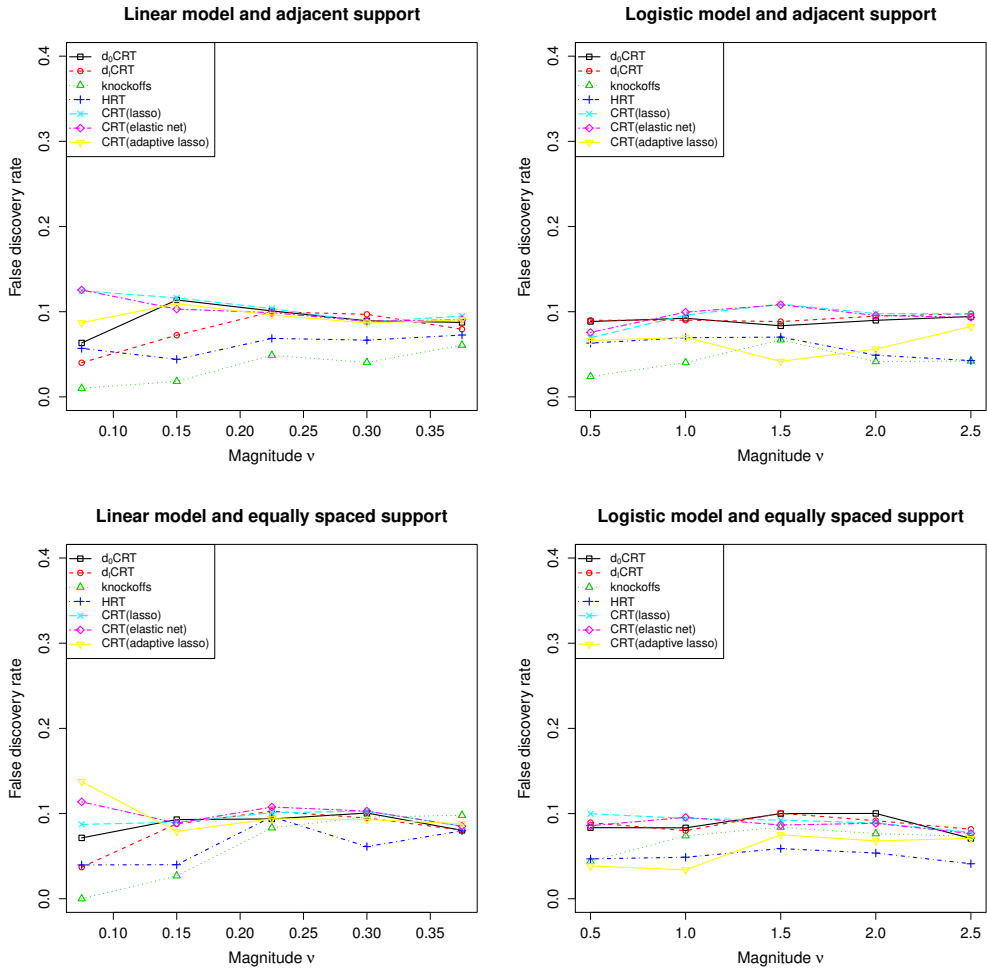


Figure A19: FDRs of the $n = p = 300$ simulation of Appendix D.2; standard errors are below 0.01. All methods control the FDR at the target level 0.1, as desired.

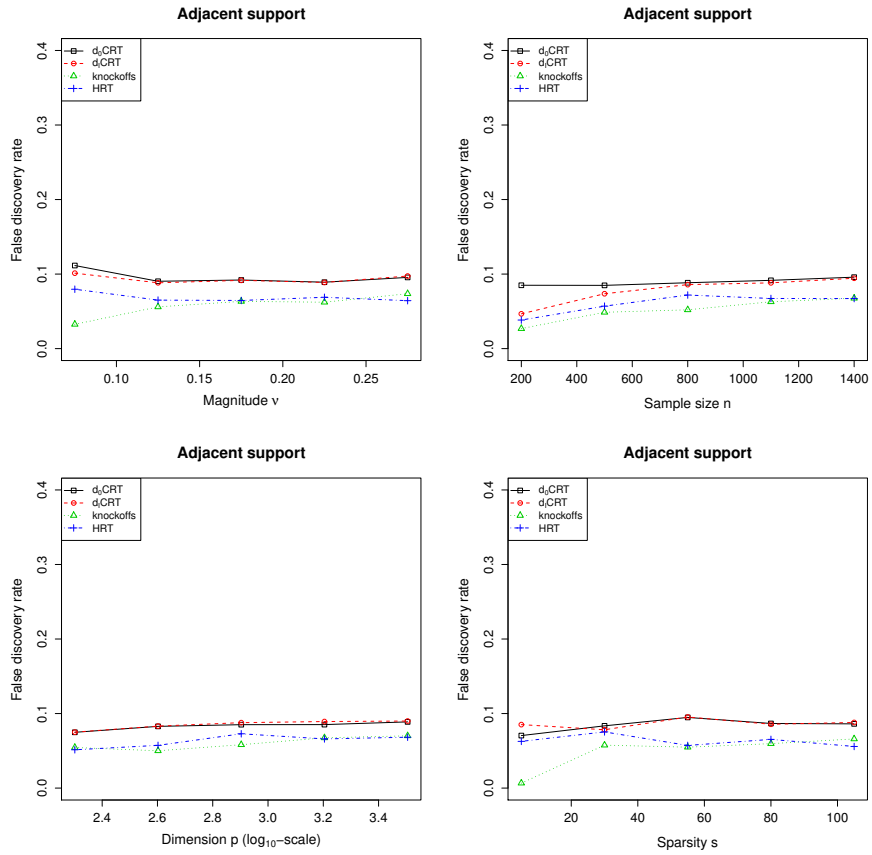


Figure A20: FDRs of the large scale simulations of Appendix D.3 that vary the coefficient magnitude, sample size, dimension, and coefficient sparsity with adjacent support. All standard errors are below 0.01; all methods control FDR across all settings, as desired.

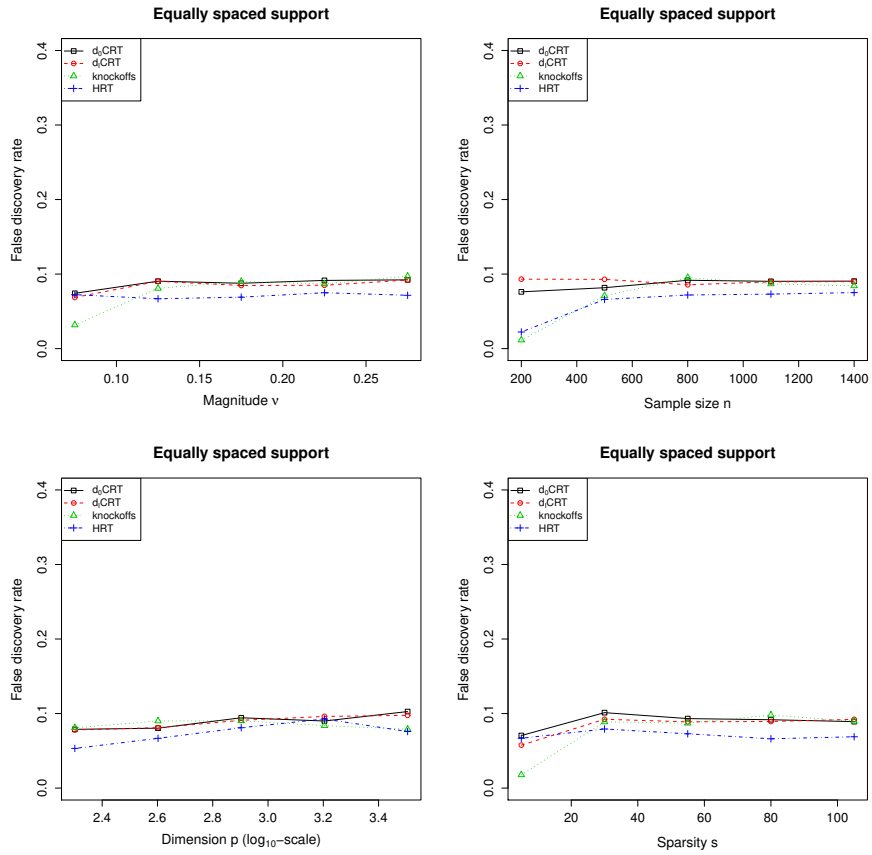


Figure A21: FDRs of the large scale simulations of Appendix D.3 that vary the coefficient magnitude, sample size, dimension, and coefficient sparsity with equally spaced support. All standard errors are below 0.01; all methods control FDR across all settings, as desired.

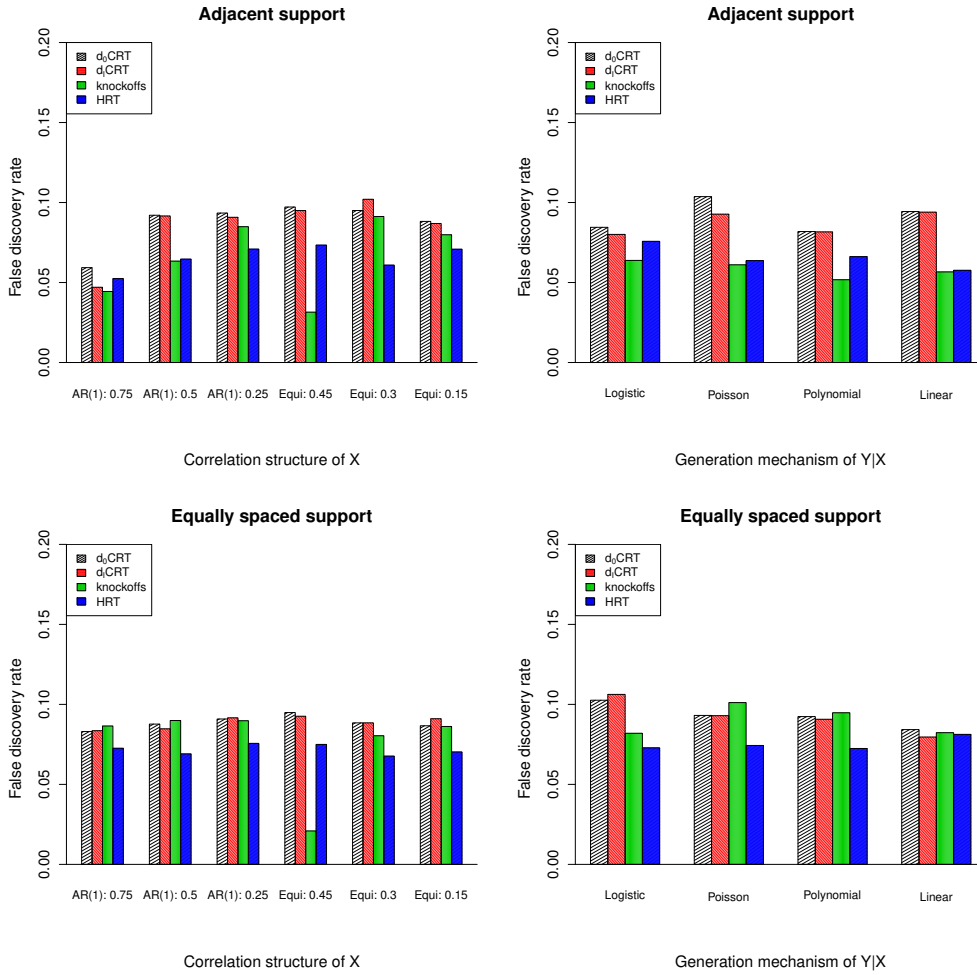


Figure A22: FDRs of the large scale simulations of Appendix D.3 that vary the covariate and response models; all standard errors are below 0.01. All methods control FDR in all settings.

E Breast cancer data analysis

In this section, we present the details of our analysis of the breast cancer data set in Section 5; our code for pre-processing and analyzing the data is available at <https://github.com/moleibobliu/Distillation-CRT>. The list of $p = 164$ candidate genes is obtained as the set of genes among those measured by Curtis et al. (2012) that are the most frequently mutated according to Pereira et al. (2016) (see Supplementary Data 1 at <https://www.nature.com/articles/ncomms11479#Sec32>). The CNA, gene expression and clinical data itself is from cBioPortal and can be downloaded from https://www.cbioportal.org/study/summary?id=brca_metabric. The raw cancer stage used in our response variable is from the column labeled *TUMOR_STAGE* in their table for clinical data. It consists of three categories, 1, 2 and 3 that represent the progression stage of breast cancer. Since there were relatively few observations in category 1, we merge categories 1 and 2 together, resulting in a binary response. And the samples for analysis were chosen as all the patients with ER+ given in the clinical table.

Now we introduce the procedures for modeling the covariates. To model the expression levels of each gene G_j conditional on its corresponding CNA level C_j , we follow the methods proposed and discussed in Solvang et al. (2011); Lahti et al. (2012); Leday et al. (2013) to fit a piecewise linear regression of each G_j on each C_j . Denoting the fitted residuals as \tilde{G}_j and $\tilde{\mathbf{G}} = (\tilde{G}_1, \dots, \tilde{G}_p)$ we then model $\tilde{\mathbf{G}}$ as mean-zero multivariate Gaussian (similar to Shen et al. (2019)) and estimate its precision matrix via a similar procedure as in Section D.8.2. That is, we remove the mean of each \tilde{G}_j , fit glasso tuned with cross-validation to estimate the precision matrix, and finally take the inverted precision matrix estimate and multiply it by a diagonal matrix to match the conditional variance of each \tilde{G}_j with the mean square of its residuals.

As in the simulations, the d_0 CRT and d_1 CRT we use are the resampling-free logistic regression versions of Examples 1 and 2 along with screening with the logistic lasso. Again, we do not use a logistic regression test statistic to allow for the computational gains of the resampling-free modification. We also implement knockoffs, the HRT, and the original CRT as in the simulations section with analogous logistic lasso statistics. The number of resamples for the HRT and the original CRT is set as $M = 25,000$, again satisfying $M/5 > p/\alpha$ as the FDR or FWER level α is set as 0.1.

We summarize the discovered genes and their p -values estimated by each method in Table A5.

Gene	d_0 CRT	d_1 CRT	CRT(lasso)	HRT
<i>FBXW7</i>	9.5×10^{-4}	3.7×10^{-4}	1.8×10^{-3}	2.0×10^{-2}
<i>GPS2</i>	2.7×10^{-4}	2.3×10^{-4}	1.2×10^{-4}	1.2×10^{-2}
<i>HRAS</i>	1.8×10^{-3}	1.9×10^{-3}	2.1×10^{-3}	5.6×10^{-4}
<i>MAP3K13</i>	4.9×10^{-5}	3.0×10^{-5}	6.1×10^{-3}	1
<i>NRAS</i>	6.0×10^{-3}	9.3×10^{-3}	7.0×10^{-3}	1.8×10^{-3}
<i>RUNX1</i>	2.5×10^{-4}	1.8×10^{-4}	2.0×10^{-4}	4.0×10^{-4}

Table A5: Selected genes and their corresponding estimated p -values; those in bold are rejected by BH at FDR level 0.1 and those underlined are rejected by Bonferroni correction at FWER level 0.1. Knockoffs selected no genes.